

# Journal of Materials Research

## Lattice Dislocation Induced Misfit Dislocation Evolution in Semi-Coherent {111} Bimetal Interfaces

--Manuscript Draft--

|  |  |                       |
|--|--|-----------------------|
| <b>Manuscript Number:</b>                            | JMRS-D-21-00017R1  |                       |
| <b>Full Title:</b>                                   | Lattice Dislocation Induced Misfit Dislocation Evolution in Semi-Coherent {111} Bimetal Interfaces   |                       |
| <b>Article Type:</b>                                 | Invited Paper  |                       |
| <b>Section/Category:</b>                             | Metal Materials  |                       |
| <b>Funding Information:</b>                          | Division of Civil, Mechanical and Manufacturing Innovation (CMMI-1761553)  | Dr. David L. McDowell |
|  | Division of Civil, Mechanical and Manufacturing Innovation (CMMI-176512)   | Dr. Youping Chen      |
| <b>Abstract:</b>                                     | <p>Characterization of misfit dislocation evolution in bimetal interfaces is critical for understanding plasticity in nanolaminates as local misfit dislocation structures affect dislocation/interface interactions. This work utilizes the Concurrent Atomistic-Continuum method to probe the evolution of misfit structures at semi-coherent Ni/Cu and Cu/Ag interfaces impinged by dislocation pileups generated via nanoindentation. A continuum microrotation metric is computed and used to visualize the evolution of the interface misfit dislocation pattern. The stress state from approaching dislocations induces mixed contraction and expansion of misfit dislocation structures. A lower misfit dislocation density coincides with greater localized deformation for atoms near misfit nodes for Ni/Cu. The increased misfit dislocation density for Cu/Ag alternatively distributes the deformation over a larger percentage of atoms at the interface. Interface sliding is found to facilitate deformation extending into the bulk lattices centered on misfit nodes. The depth of penetration of those fields is greater for Ni/Cu than for Cu/Ag.</p> |                       |
| <b>Corresponding Author:</b>                         | Alex Selimov<br>Georgia Institute of Technology School of Materials Science and Engineering<br>UNITED STATES   |                       |
| <b>Corresponding Author Secondary Information:</b>   |  |                       |
| <b>Corresponding Author's Institution:</b>           | Georgia Institute of Technology School of Materials Science and Engineering  |                       |
| <b>Corresponding Author's Secondary Institution:</b> |  |                       |
| <b>First Author:</b>                                 | Alex Selimov   |                       |
| <b>First Author Secondary Information:</b>           |  |                       |
| <b>Order of Authors:</b>                             | Alex Selimov   |                       |
|  | Shuozhi Xu   |                       |
|  | Youping Chen   |                       |
|  | David L. McDowell  |                       |
| <b>Order of Authors Secondary Information:</b>       |  |                       |
| <b>Author Comments:</b>                              |  |                       |
| <b>Response to Reviewers:</b>                        | Please view the attached response to reviewers letter in the manuscript for responses to all reviewer comments.  |                       |
| <b>Suggested Reviewers:</b>                          | Shuai Shao<br>szs0244@auburn.edu<br>Has direct expertise with modeling of semi-coherent interfaces.  |                       |

Caizhi Zhou  
caizhi@mailbox.sc.edu  
Has a strong background in modeling of nanolaminate materials and multi-scale modeling.

Xiang Chen  
shawnc@latech.edu  
Expertise in CAC modeling and has worked on studying interfaces utilizing CAC.

[Click here to view linked References](#)

# Lattice Dislocation Induced Misfit Dislocation Evolution in Semi-Coherent {111} Bimetal Interfaces

Alex Selimov<sup>1</sup>, Shuozhi Xu<sup>2</sup>, Youping Chen<sup>3</sup>, and David McDowell<sup>1,4</sup>

The study of dislocation plasticity mediated by semi-coherent interfaces can aid in the design of certain heterostructured materials, such as nanolaminates. The evolution of interface misfit patterns under complex stress fields arising from dislocation pileups can influence local dislocation/interface interactions, including effects of multiple incoming dislocations. This work utilizes the Concurrent Atomistic-Continuum modeling framework to probe the evolution of misfit structures at semi-coherent Ni/Cu and Cu/Ag interfaces impinged by dislocation pileups generated via nanoindentation. A continuum microrotation metric is computed at various stages of the indentation process and used to visualize the evolution of the interface misfit dislocation pattern. The stress state from approaching dislocations induces mixed contraction and expansion of misfit dislocation structures at the interface. A lower number of misfit nodes per unit interface area coincides with greater localized deformation with regard to atoms near misfit nodes for Ni/Cu. The decreased misfit node spacing for Cu/Ag alternatively distributes the restructuring associated with plastic deformation over a larger percentage of atoms at the interface. Interface sliding facilitated by misfit dislocation motion is found to facilitate deformation extending into the bulk lattices centered on misfit nodes. The depth of penetration of those fields is found to be greater for Ni/Cu than for Cu/Ag.

[Abstract figure: FIG 8]

<sup>1</sup> Department of Materials Science and Engineering, Georgia Institute of Technology, Atlanta, GA, 30332

<sup>2</sup> Department of Mechanical Engineering, University of California, Santa Barbara, CA, 93106

<sup>3</sup> Department of Mechanical and Aerospace Engineering, University of Florida, Gainesville, FL, 32611

<sup>4</sup> Woodruff School of Mechanical Engineering, Georgia Institute of Technology, Atlanta, GA, 30332

## Introduction

Heterostructured materials are characterized by heterogeneous domains with significantly different material properties that interact cooperatively to improve overall mechanical behavior. These heterogeneous domains consist of multi-modal or graded distributions of grain size [1, 2], texture [3], or phase [4, 5, 6]. One particular heterostructured material which has garnered much interest is the nanolaminate, which consists of alternating phases in a lamellar structure with layer thicknesses in the range of several to tens of nm. They exhibit improved properties compared to their bulk constituents [7, 8, 9] due to the mediating influence of interphase boundaries on dislocation absorption, desorption, or direct transmission. These interfaces mediate the transmission of plastic deformation between layers, depending on the interface structure [10, 11]. The influence of complex stress states, such as those induced by approaching dislocations, can impact interface misfit

1  
2  
3  
4 patterns [12]. Changes to interface misfit dislocation spacing, resulting from applied shear  
5 stress [13, 14], has been shown to change various aspects of interface structure and energy  
6 minimization processes [15]. This can contribute to the interface blocking strength through  
7 increased misalignment of slip planes [16] or by increased misfit dislocation density at the  
8 lattice dislocation impingement [17]. Computational methods are necessary to explore  
9 such complexities of interface evolution during plastic deformation, since *in situ*  
10 transmission electron microscopy is difficult to perform [18].  
11  
12

13  
14 The evolution of semi-coherent interface structures during dislocation transmission  
15 and/or restructuring under loading has previously been investigated using atomistic  
16 methods. Shao et al. [19] studied the energy minimized spiral patterns of misfit dislocations  
17 entering misfit dislocation junctions, referred to as “nodes,” in the Ni/Cu system and found  
18 that the expansion and contraction of the nodal structures under mechanical shearing  
19 affected their ability to absorb and emit point defects. Asymmetrical non-Schmid  
20 nucleation of dislocations from misfit node structures in Ni/Cu semi-coherent interfaces  
21 under various in plane boundary conditions was found by Chen et al. [14], revealing the  
22 inherent heterogeneity of these interfaces and the need for atomic resolution to capture  
23 evolution of interface plasticity. Interface sliding, facilitated by migration of misfit  
24 dislocations along the interface plane, was explored for the Ni/Cu system by Chen et al.  
25 [14] and for the Ni/Ni<sub>3</sub>Al system by Yang et al. [20] through molecular dynamics (MD)  
26 simulations. These studies lead to the conclusion that the misfit nodes initiate plastic  
27 deformation under loading, either by acting as a dislocation source or facilitating interface  
28 sliding under applied shear stress. Changes to interface energy minimization pathways for  
29 different misfit node spacings has been studied for Ni/Cu and Cu/Ag systems by Shao et al.  
30 [21], who found that the degree of spiraling at misfit nodes is controlled by the misfit node  
31 spacing. This implies that misfit dislocation pattern evolution under loading may occur  
32 along different pathways for different misfit node spacings. However, these atomistic  
33 studies on semi-coherent interfaces are generally limited to either a single misfit node or a  
34 small number of misfit nodes for relatively small computation cells with periodic boundary  
35 conditions applied within the interface plane and homogeneous stress/deformation states  
36 applied to the cell boundary. This accordingly limits or constrains the range of misfit  
37 pattern evolution observed. Discussion of models with larger interfaces that contain more  
38 misfit nodes is lacking in the literature, likely due to the characteristic length-scale of the  
39 misfit pattern associated with some common interfaces, such as the interface between  
40 Ni/Cu [20], and complex energy landscapes which require many iterations for  
41 convergence. Both factors make atomistic studies difficult due to computational costs.  
42 However, such studies are essential when considering highly heterogeneous interface  
43 stress fields associated with dislocation pileup impingement; this phenomenon is generally  
44 beyond the capability of small periodic cell sizes used in full MD simulations.  
45  
46  
47  
48  
49  
50  
51  
52

53 To facilitate studies of larger interface sections and the evolution of their misfit patterns in  
54 the presence of shear gradients, we consider a fully concurrent approach to coarse-graining  
55 of atomistics. In this regard, we mention the coarse-graining Quasi-Continuum (QC)  
56 method and variants [22, 23] and the domain decomposition-based Coupled Atomistic  
57 Discrete Dislocation method [24, 25]. The interested reader can consult prior reviews of  
58 these schemes for concurrent multiscale modeling of dislocation reactions [26, 27, 28]. We  
59  
60  
61  
62  
63  
64  
65

1  
2  
3  
4 employ instead the Concurrent Atomistic-Continuum (CAC) [29] method in the present  
5 study, as it can address the migration and exchange of arrays of dislocations in coarse-  
6 grained and fully resolved atomistic regions without adaptive mesh refinement, does not  
7 require any constitutive relation beyond the interatomic potential, and avoids domain  
8 decomposition based on different constitutive models and associated transfer of  
9 information across domains. Accordingly, it efficiently captures long range fields in the  
10 lattice using usual nonlocal atomistics, while allowing fully resolved dislocation-defect  
11 reactions. Coarse-graining is achieved in bulk regions to reduce degrees of freedom, while  
12 full atomistic resolution is maintained within regions that undergo large extent of atomic  
13 restructuring to ensure the accuracy of the reaction pathway. Dislocations are  
14 accommodated naturally along interelement discontinuities, fully capturing long range  
15 elastic fields [30] and reducing the required degrees of freedom for modeling dislocation  
16 arrays. Dislocations seamlessly pass between coarse-grained regions and atomistic regions  
17 along the discontinuities in the finite element mesh without requiring heuristics to transfer  
18 dislocation information between regions. CAC has been applied to a variety of problems  
19 which require extended domains to model inhomogeneous structure evolution. Dislocation  
20 pileups and their interactions with a variety of obstacles have been studied including void  
21 and inclusion bypass [31]. Models of approximately 86 million equivalent atoms (42,000  
22 finite elements) have been used to study the nucleation, growth, and interaction of  
23 dislocation loops in Cu, Al, and Si [32]. Of particular relevance to the current research are  
24 studies on the transmission of dislocations across coherent twin boundaries in Cu and Al  
25 [33], coherent twin boundaries and symmetric tilt grain boundaries in Ni [34], and Si/Ge  
26 semi-coherent interfaces [35], as well as on semi-coherent interface structures in  
27 PbTe/PbSe bilayers with semi-coherent interfaces [36]. All these studies utilized the mesh  
28 discontinuity to accommodate dislocations, reducing required degrees of freedom far from  
29 the interface, while maintaining the interfaces at full atomistic resolution. As such, it was  
30 possible to observe the interaction of dislocation arrays with interfaces and the evolution  
31 of the interface structure with simulation domains approaching the micron scale. The  
32 largest CAC model to date employed over 10 billion atoms [37]. These types of problems  
33 are intractable for atomistic methods due to the required domain sizes. Other types of  
34 concurrent multiscale methods such as the QC method may struggle as the interactions  
35 between these defect arrays and extended interface dislocations may require adaptive  
36 remeshing to full atomistic resolution over much of the domain.

37  
38  
39  
40  
41  
42  
43  
44  
45  
46 In this work, periodic energy minimization is utilized in a so-called quasistatic CAC ap-  
47 proach [30] to assess the near-equilibrium lattice dislocation induced misfit pattern evolu-  
48 tion that is typical of thermally-assisted deformation. This avoids the high effective strain  
49 rates associated with MD which can result in aphysical overdriven reactions [38]. **Entropic**  
50 **effects are not considered in this work. To study thermally activated processes, quasistatic**  
51 **simulations should minimally be augmented with harmonic transition state theory [39, 40]**  
52 **or use of the Meyer-Neldel compensation law to estimate activation entropy [41, 42] based**  
53 **on activation enthalpy of dislocation-interface reactions computed, for example, using**  
54 **nudged elastic band (NEB) methods [43]. Studying the mechanically induced misfit pattern**  
55 **evolution under quasi-static conditions prior to interactions with lattice dislocations can**  
56 **more realistically inform reduced order models, as the local misfit dislocation environment**  
57 **is known to affect slip transmission [17, 35] and is not too far from equilibrium. Capturing**  
58  
59  
60  
61  
62  
63  
64  
65

this evolution necessitates the use of large interface segments to allow for non-uniform misfit structure evolution. Important implications regarding the interface misfit structure stability and interface shear strength can furthermore aid in the design of interfaces used for hierarchically structured nanolaminates.

### Non-uniform interface sliding under complex stress fields ahead of dislocation pileups

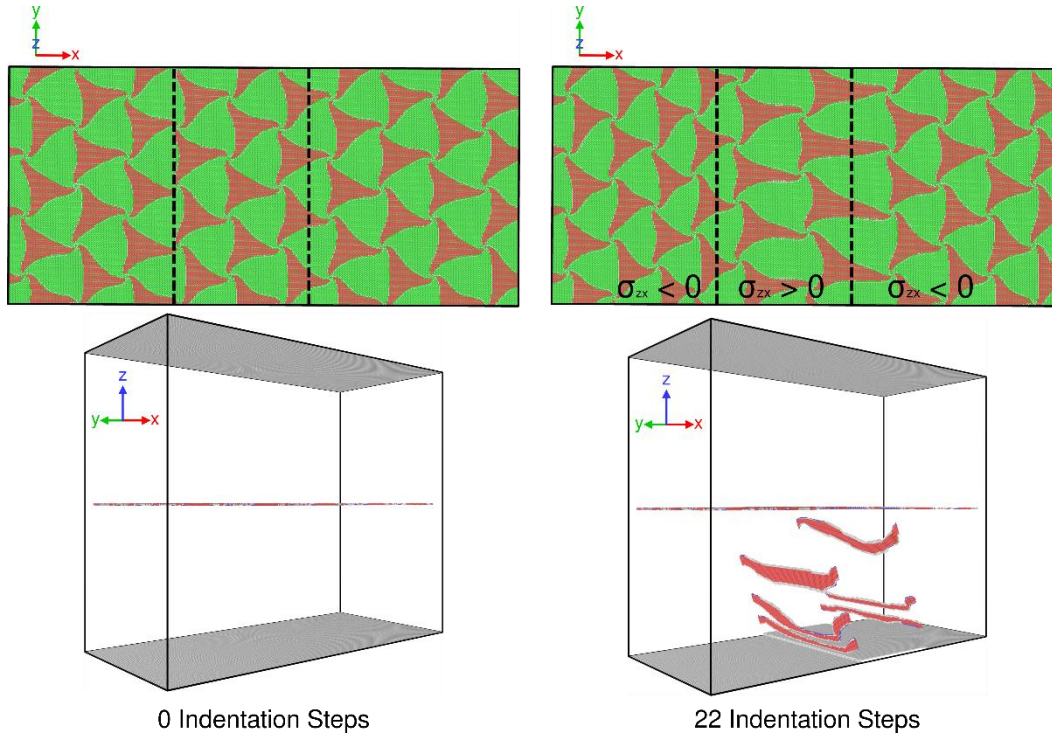


Figure 1: Common neighbor analysis for all atoms at interface (top) and with FCC atoms hidden (bottom) at two different indentation steps for Ni/Cu. Red atoms are in an HCP structure, blue atoms are in a BCC structure and gray atoms are in undefined structures. Deformation of misfit structures occurs as heterogeneous compression/extension of the nodal spacing in the  $x$  direction. Dashed lines in the top figures represent the impingement line of the incoming dislocations on the interface.

The first stage in the interface misfit dislocation pattern evolution with the approach of the lead dislocation in each pileup is the motion of misfit dislocations and their junctions, referred to as “nodes.” It is known that under shear loading conditions, semi-coherent interfaces can exhibit interface sliding via the motion of misfit dislocations along the interface plane [14, 20, 35]. Interface sliding generally originates in the misfit nodes as they readily glide under shear conditions in bimetal semi-coherent interfaces, such as Ni/Cu and Cu/Ag. A shear stress induced by indentation generated dislocations drives the evolution of misfit patterns for the investigated geometries, as seen for Ni/Cu in Figure 1 where the projected impingement of the dislocation pileup slip planes are denoted by dotted lines. These lines separate the regions of the interface which are on the compressive side of the incoming dislocations and the portions of the interface which are on the tensile side. This

results in sharp  $\sigma_{zx}$  shear stress gradients at the impingement lines that cause the non-uniform expansion/contraction of the misfit patterns. This is more pronounced in the Ni/Cu interface than in the Cu/Ag interface. The evolution of the misfit node position in the  $x$  direction helps to illustrate this behavior and is presented in Figure 2. The dislocation nodes in the Ni/Cu interface are repulsed primarily from the rightmost pileup impingement line in the interface because dislocations progress first along the right edge of the indenter, as seen in Figure 1. By comparison, only relatively small shifts in misfit node position are observed for the Cu/Ag interface.

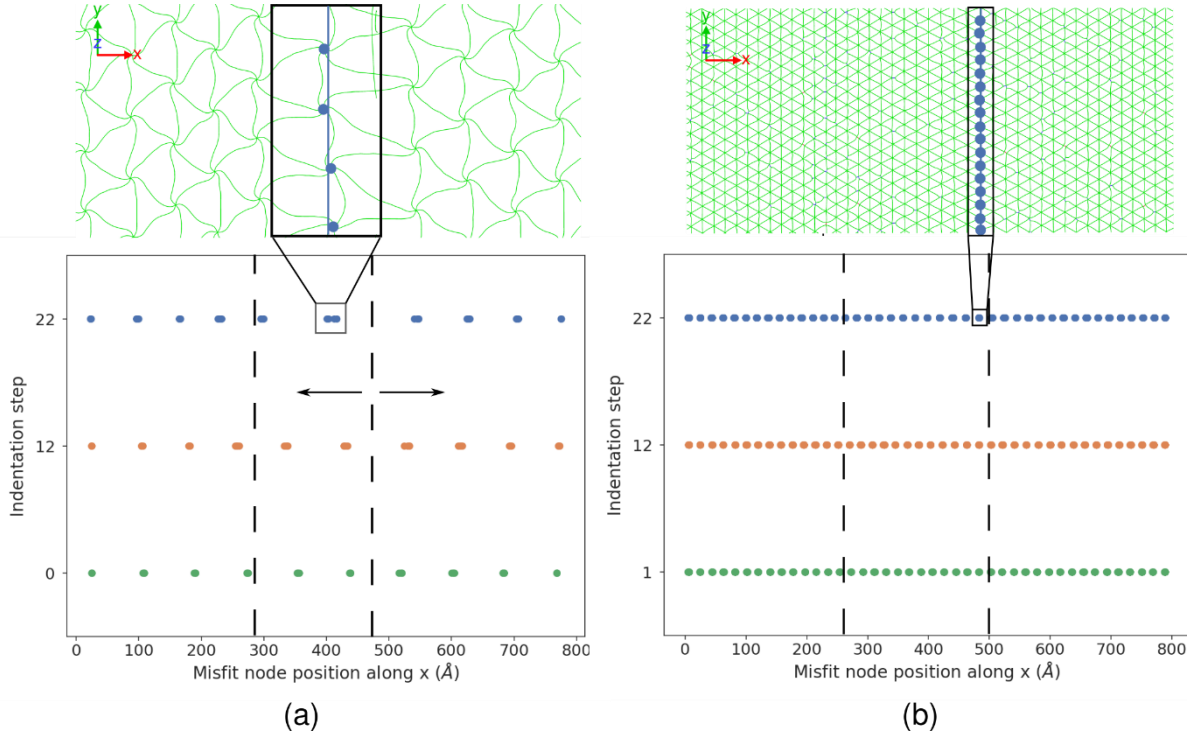


Figure 2: Position of dislocation nodes along  $x$  direction for 3 different time steps for a) Ni/Cu and b) Cu/Ag. Dashed lines represent the slip plane impingement lines. Multiple nodes at the interface have very close  $x$ -positions due to the misfit periodicity in the current orientation as shown in the exploded view. The arrows indicate the direction of misfit node motion away from the impingement line. Colors denote different indentation steps.

This differences in the evolution of misfit patterns can be attributed primarily to the misfit dislocation spacing. Smaller regions of coherency at the Cu/Ag interface reduces the distance that dislocations can freely glide, while the increased density of misfit nodes serves to block the motion of other misfit dislocations or nodes. For motion to occur it must occur cooperatively over larger portions of the interface. Decreasing misfit node spacing for the Ni/Cu interface, for example by twisting one of the crystals relative to the other [21], is expected to lead to increased misfit structure stability. It is also important to note that the motion of misfit nodes is away from the incoming lattice dislocation. It is expected that misfit nodes would be strong obstacles to slip transmission due to their low shear

1  
2  
3  
4 strength which could promote dislocation core spreading within the interface plane.  
5 Decreased misfit spacings have been found to result in increased resistance to slip transfer  
6 [35]. Because the Cu/Ag interface is more stable, this motion of misfit nodes does not occur  
7 over significant distances and interactions of incoming lattice dislocations with misfit  
8 nodes are more likely, possibly contributing to further increases in blocking strength. In the  
9 case of sessile misfit nodes, such as in metal/ceramic semi-coherent interfaces [43],  
10 dislocations will bow out in opposite directions, depending on the sign of the induced shear  
11 stress, with dislocation segments pinned by the misfit nodes. The degree to which the  
12 dislocations bow out will increase as additional dislocations are generated in the pileup.  
13 This type of spatially varying interface structure evolution is generally missed in atomistic  
14 methods due to low number of misfit nodes modeled resulting from limitations in the size  
15 of interface sections which can be modeled.  
16  
17  
18  
19

## 20 Effects of misfit node spacing on the evolution of misfit dislocation patterns

21  
22 The microrotation is used to quantitatively characterize the nature of the interface  
23 deformation as components of the microrotation vector can capture different aspects of the  
24 deformation, as shown in Figure 3 for Ni/Cu and in Figure 4 for Cu/Ag. Because the misfit  
25 dislocations are constrained to the  $x$ - $y$  interface plane, the first component of the  
26 microrotation captures the local rotations associated with motion of dislocations in the  $y$   
27 (or [011]) direction and the second component captures the motion of dislocations in the  $x$   
28 (or  $[\bar{2}1\bar{1}]$ ) direction; these microrotation components register relative rotation of atoms  
29 across the interface plane. The third component of the microrotation captures both and is  
30 not presented due to its lack of specificity in this regard.  
31  
32  
33  
34

35 At earlier indentation steps, as seen for Ni/Cu in Figure 3, the microrotation fields are  
36 primarily concentrated at the misfit nodes with some degree of spreading along misfit  
37 dislocation lines. As stress increases due to the indentation, the microrotation fields begin  
38 to increase in magnitude in the coherent and stacking fault portions of the interface. This  
39 indicates that the interface deformation begins at the misfit nodes, proceeds along the  
40 misfit dislocation lines, and through misfit dislocation glide to the rest of the interface.  
41 Local differences in the sense of the microrotation, seen as alternating blue and red fields,  
42 relates to the non-uniform local rotation of the lattice structure required for unidirectional  
43 misfit node motion in Ni/Cu [14]. Misfit nodes which display these alternating  
44 microrotation fields experience little net movement in the [011] direction, suggesting that  
45  
46  
47

48 the  $\sigma_{zy}$  component of the shear stress is small. At these earlier stages, the development of  
49 the first microrotation component can be attributed primarily to restructuring required for  
50  
51

52 motion of the misfit nodes in the  $[\bar{2}1\bar{1}]$  direction. This non-uniform misfit dislocation glide  
53 which is seen to accompany the misfit node motion does however result in a change to the  
54 spacing of the dislocation lines at their points of intersection with the incoming lattice  
55 dislocation slip planes. Coherent FCC regions near the impingement lines grow in size while  
56 the stacking fault regions shrink, causing both expansion/contraction to the dislocation  
57 intersection point spacing along the impingement line. Maximum observed changes  
58 approached 9 Å. The literature shows that the misfit dislocation spacing affects slip  
59  
60  
61  
62  
63  
64  
65



transmission [35]. This type of evolution of misfit structures ahead of incoming lattice dislocations may therefore be non-negligible when considering slip transmission. The second component of the microrotation shows a shift in the direction of lattice rotation which accompanies misfit node motion when crossing the rightmost dislocation impingement line. This shift in the sense of the microrotation is associated with the opposite signs of  $\sigma_{zx}$  on either side of the line which drives the motion of misfit nodes in opposite directions.

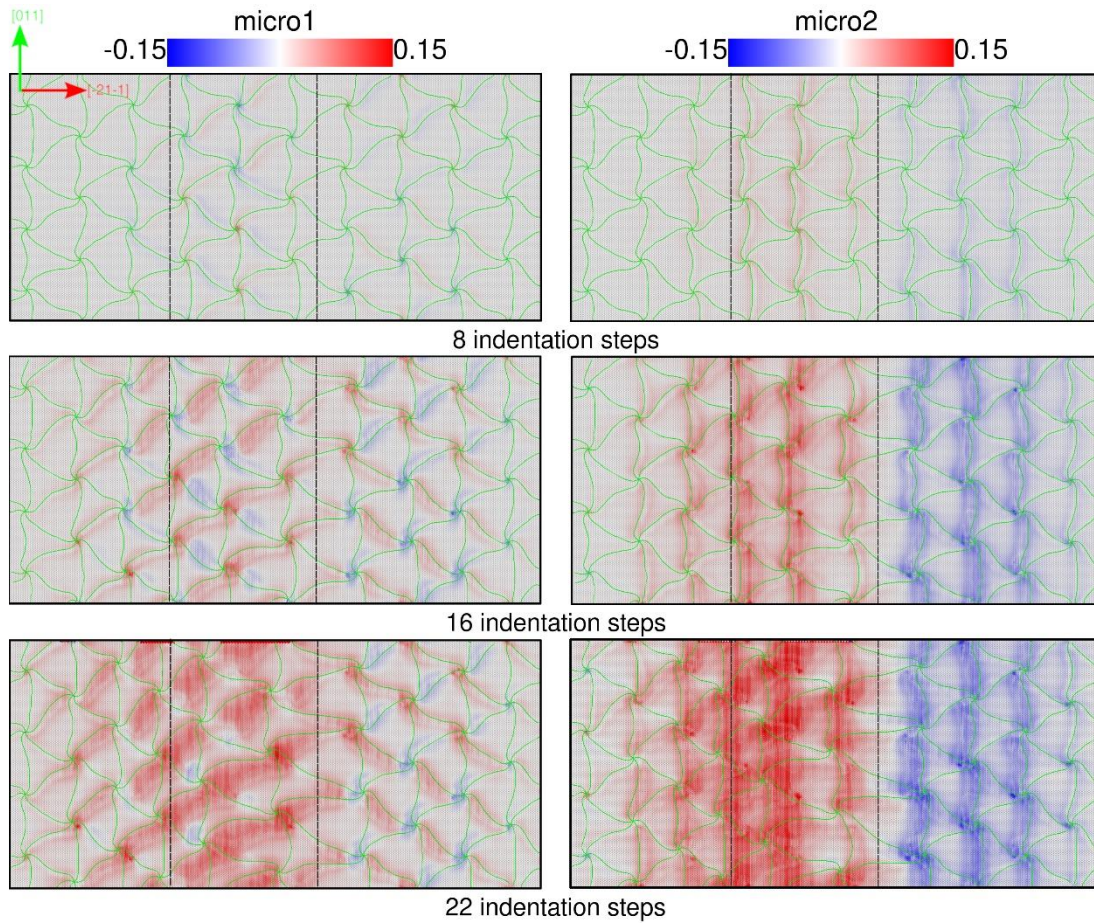
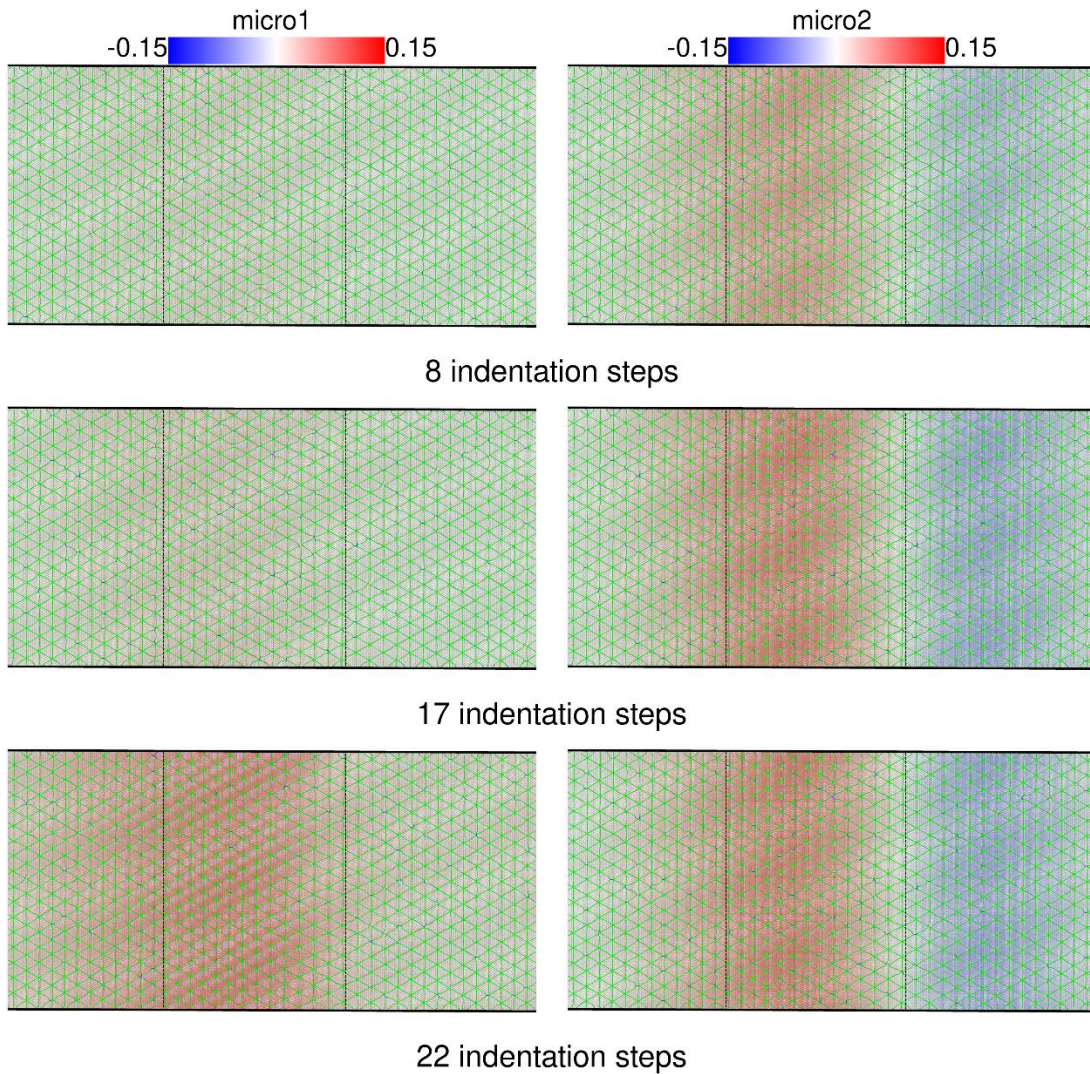


Figure 3: The first (micro1) and second (micro2) components of the microrotation vectors at various indentation steps for the Ni atoms at the Ni/Cu interface. It is seen that at earlier indentation steps the microrotation is maximized at the misfit nodes and then increases along the dislocation lines as indentation progresses.

The microrotation fields at the Cu/Ag interface presented in Figure 4 have similar overall patterns to those of Ni/Cu, indicating that the global motion of misfit nodes occurs along the same directions. Lower magnitudes for both components of the microrotation are seen as lower intensities for Cu/Ag and suggest a lower misfit node mobility within the interface. The regions with alternating sense for the first component of the microrotation, observed for Ni/Cu, are missing for Cu/Ag. This implies that the net motion of misfit nodes in the  $[\bar{2}1\bar{1}]$  direction does not require local rotation of the atomic structure about the

1  
2  
3  
4 [011] direction. The spiraling of misfit dislocations as they enter the misfit nodes, seen in  
5 Ni/Cu but not observed for Cu/Ag, may be the cause for this difference. Maintaining the  
6 spiral pattern at the misfit nodes may require larger deviations from the equilibrium lattice  
7 structure when compared to the motion of straight dislocation segments in Cu/Ag.  
8 Smoother fields are also observed, which indicates the increased participation of atoms  
9 at the interface in the deformation for Cu/Ag due to the increased percentage of atoms in the  
10 vicinity of misfit dislocations and misfit nodes (the number density of nodes in the  
11 interface plane is higher). The higher magnitudes and comparatively lack of smooth fields  
12 for the microrotation observed in Ni/Cu arise from the lower percentage of atoms in the  
13 vicinity of misfit dislocations and misfit nodes.  
14  
15  
16



54 *Figure 4: The first (micro1) and second (micro2) components of the microrotation vectors at*  
55 *various indentation steps for the Cu atoms at the Cu/Ag interface. Smoother fields of*  
56 *microrotation are evident when compared to those found in the Ni/Cu interface, shown in*  
57 *Figure 3.*  
58  
59  
60  
61  
62  
63  
64  
65

1  
2  
3  
4 The misfit node spacing therefore affects the interface deformation in two primary ways.  
5 First, the misfit node spacing controls the stability of the interface structure. A decreased  
6 misfit node spacing results in a more uniform distribution of deformation across interface  
7 atoms. The misfit dislocations and misfit nodes under the same shear stress condition glide  
8 in the same direction. This is observed by the smooth microrotation fields and the uniform  
9 sense of the microrotation for atoms on the same sides of the incoming dislocation  
10 impingement lines. Alternatively, the larger misfit dislocation spacings of Cu/Ni exhibit  
11 significant deformation of the misfit dislocation structure, including changes to misfit  
12 dislocation spacing along the impingement lines resulting from misfit dislocation glide in  
13 variant directions. These changes to the misfit structure of Ni/Cu may cause decreases to  
14 the slip transmission resistance of the interface. Second, in addition to significant  
15 distortions of the misfit patterns, localization of deformation is observed. This arises due to  
16 the decreased number of atoms in the vicinity of misfit dislocations which participate in the  
17 misfit pattern evolution. This is observed by the strongly concentrated microrotation fields  
18 which are concentrated at the misfit dislocations and misfit nodes.  
19  
20  
21  
22

## 23 24 **Quantitative analysis of interface deformation through microrotation** 25 **distributions** 26

27  
28 To better quantify these differences in misfit pattern evolution, the fraction of atoms  
29 containing different microrotation component values is presented in Figure 5. This is done  
30 by binning the microrotation component magnitudes for atoms within 2 nm of the interface  
31 and then normalizing the number of atoms with a specific microrotation component  
32 magnitude by the total number of atoms in all bins. For all plots, at lower indentation steps  
33 the microrotation values are narrowly distributed around zero. As the dislocation  
34 approaches the interface, the distribution of  $\phi_2$  begins to broaden symmetrically with an  
35 associated drop in the number of atoms reporting zero microrotation. The tails of the  
36 distribution for Cu/Ag tend to hold higher fractions of atoms than the tails of the  
37 distribution for Ni/Cu which drop to zero more rapidly. This quantitatively shows that  
38 decreased misfit node spacing results in a more uniform distribution of deformation across  
39 the interface.  $\phi_1$  shows a similar broadening of the distribution and a drop in the number  
40 of atoms experiencing zero microrotation but with a skew to positive values at larger  
41 timesteps. The increased symmetry observed for the distribution of this component for  
42 Ni/Cu relates to the more complex rotation of the atomic structure around misfit nodes  
43 required for accommodating the motion of the spiral patterned misfit dislocations.  
44  
45  
46  
47  
48  
49  
50  
51  
52  
53  
54  
55  
56  
57  
58  
59  
60  
61  
62  
63  
64  
65

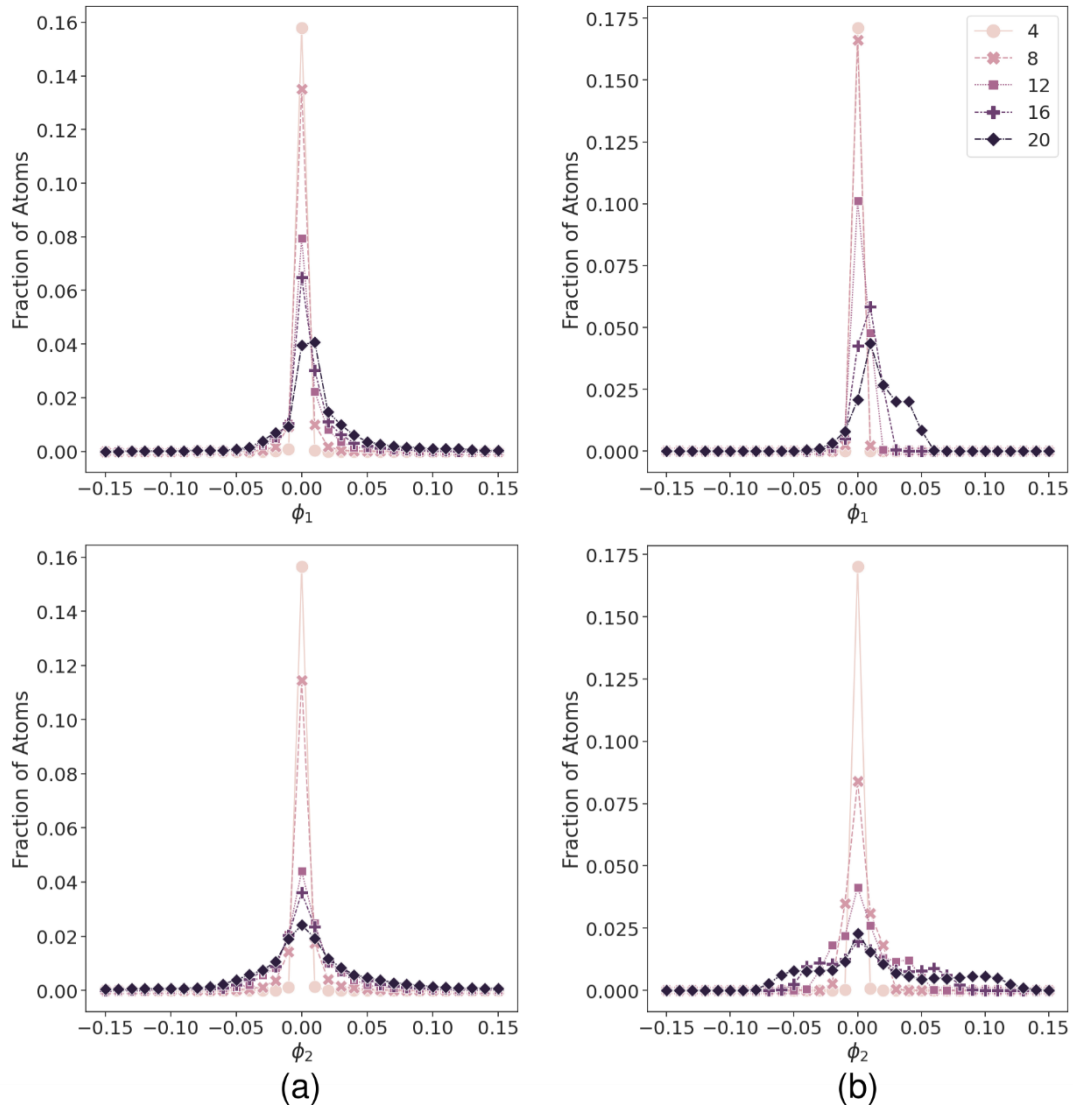


Figure 5: Binned microrotation versus frequency for a) Ni/Cu and b) Cu/Ag. For both systems,  $\phi_2$  is distributed symmetrically around 0 with a slight skew to positive values.  $\phi_1$  shows a clear skew to positive values and is more equally distributed at higher values for Cu/Ag.

Figure 5 may give the impression that the Cu/Ag interface experiences greater deformation of misfit patterns when compared to Ni/Cu due to the higher number of atoms that experience larger microrotation fields. However, calculating the maximum value for the microrotation of atoms at the interface for both systems shows higher maximum microrotation values for Ni/Cu at every timestep, as seen in Figure 6. These maximum values are also multiple factors larger than the average microrotations calculated for the Ni/Cu interface, as seen from Figure 5. This is indicative of large deviations in deformation experienced by interface atoms and the localization of plasticity to small regions of atoms around misfit nodes. In the case of Cu/Ag, the maximum values are much closer to the average microrotation for atoms at the interface, which indicates a more uniform distribution of deformation. Magnitudes for microrotation of approximately 0.15 indicate

full slip and magnitudes of 0.09 indicate partial slip associated with atoms located in a stacking fault separating partial dislocations [44]. The maximum values of microrotation for Cu/Ag indicate that at most a local atomic neighborhood at the interface has undergone full slip whereas the maximum values for Ni/Cu, well above 0.15, suggest larger and more complex degree of restructuring.

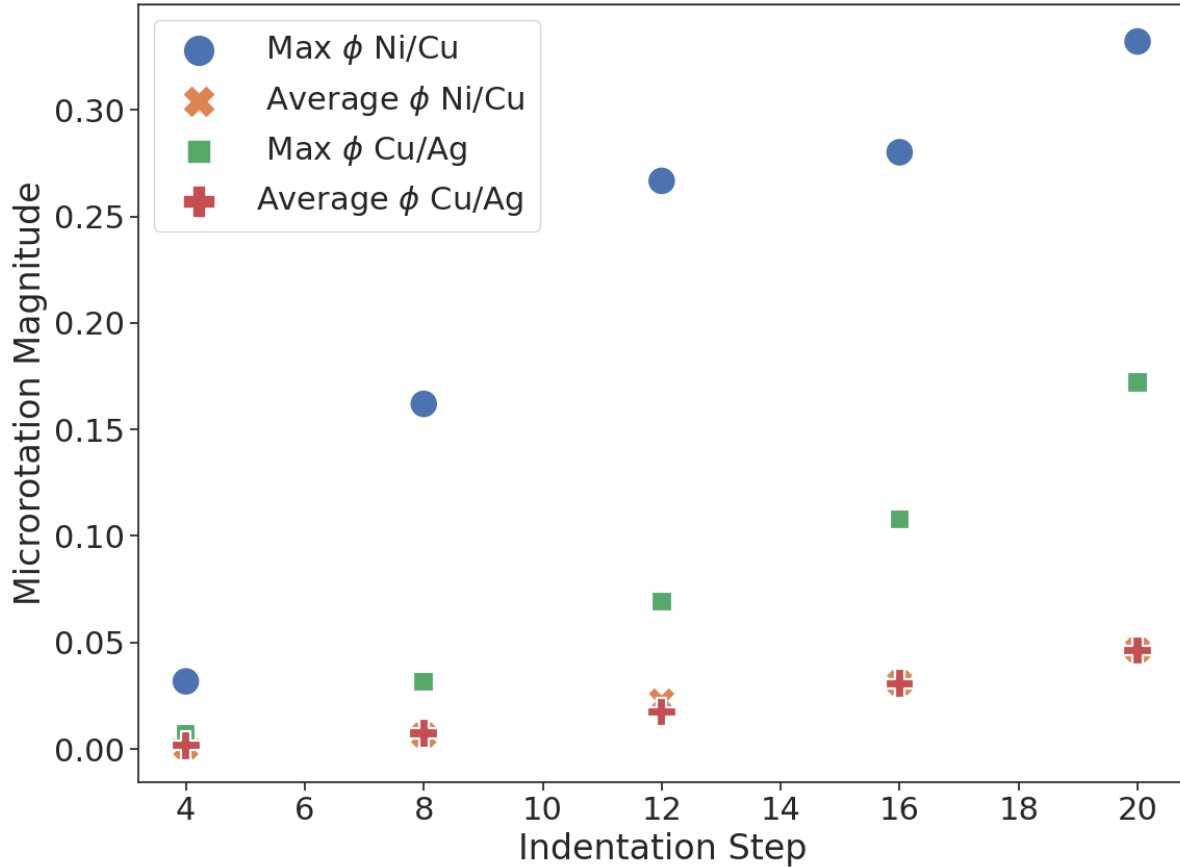


Figure 6: Maximum and average microrotation magnitudes for atoms near the interface. Larger maximum magnitudes are measured for Ni/Cu, but average values are similar for both interfaces; this suggests similar total amounts of interface deformation occurs, but with increased localization for Ni/Cu.

In summary, through the numerical analysis of the microrotation fields it is evident that localization of plasticity occurs to a larger degree for the Ni/Cu interface. The distributions of microrotation magnitudes among interface atoms confirm this as seen by a narrower distribution of microrotations for Ni/Cu than for Cu/Ag. The larger ratio of maximum microrotation magnitude to average microrotation magnitude provides additional validation of this conclusion.

## Deformation fields extend from misfit nodes and can be characterized through the microrotation

Associated with misfit dislocation motion is a deformation field that extends into the bulk lattice. This is also evident from the microrotation, where “islands” containing regions of atoms which have undergone deformation extend from the misfit nodes at the interface; this is shown in Figure 7a for Ni/Cu and Figure 7b for Cu/Ag. These islands grow in size and magnitude as the indentation progresses, extending further into both bulk lattices. The extended deformation fields originating at the misfit nodes agree with previous findings that misfit nodes serve as dislocation nucleation sites for the Ni/Cu semi-coherent interface [13, 14]. Extended microrotation fields from grain-boundaries have previously been associated with dislocation nucleation from those boundaries [44]. These microrotation fields penetrate deeper into the bulk lattices for the Ni/Cu interface than for the Cu/Ag interface, which is indicative of extended deformation of the crystal lattice as a result of the change of configuration of the misfit dislocations. To quantify the extent that these fields grow into the bulk layer, the atoms are binned along the  $z$  direction in bins of approximately 2 Å thickness. The average microrotation magnitude for atoms within the bin is then calculated and compared for Ni/Cu and Cu/Ag in Figure 7.

Magnitudes of both microrotation components tend to approach similar values far from the interface. The Ni/Cu microrotation fields decay over larger distances than the measured Cu/Ag fields, indicating that the significant motion of misfit dislocations must be accommodated by deformation of the atomic structure in neighboring planes. Similar extended deformation fields associated with the interface restructuring that occurs upon minimization of the unrelaxed interface structure, as seen in [19], are likely the primary source of error measured in the mesh sensitivity study presented in the Methodology section and Figure 9. This error arises from the constraint imparted by the coarse-graining scheme which is not able to fully capture the non-linear deformation fields. In the studied geometries, the atomistic region was large enough to fully capture this extended lattice restructuring. The reader can refer to the Methodology section for a more in-depth discussion of error introduced by the distance of the interface to the coarse-grained region.

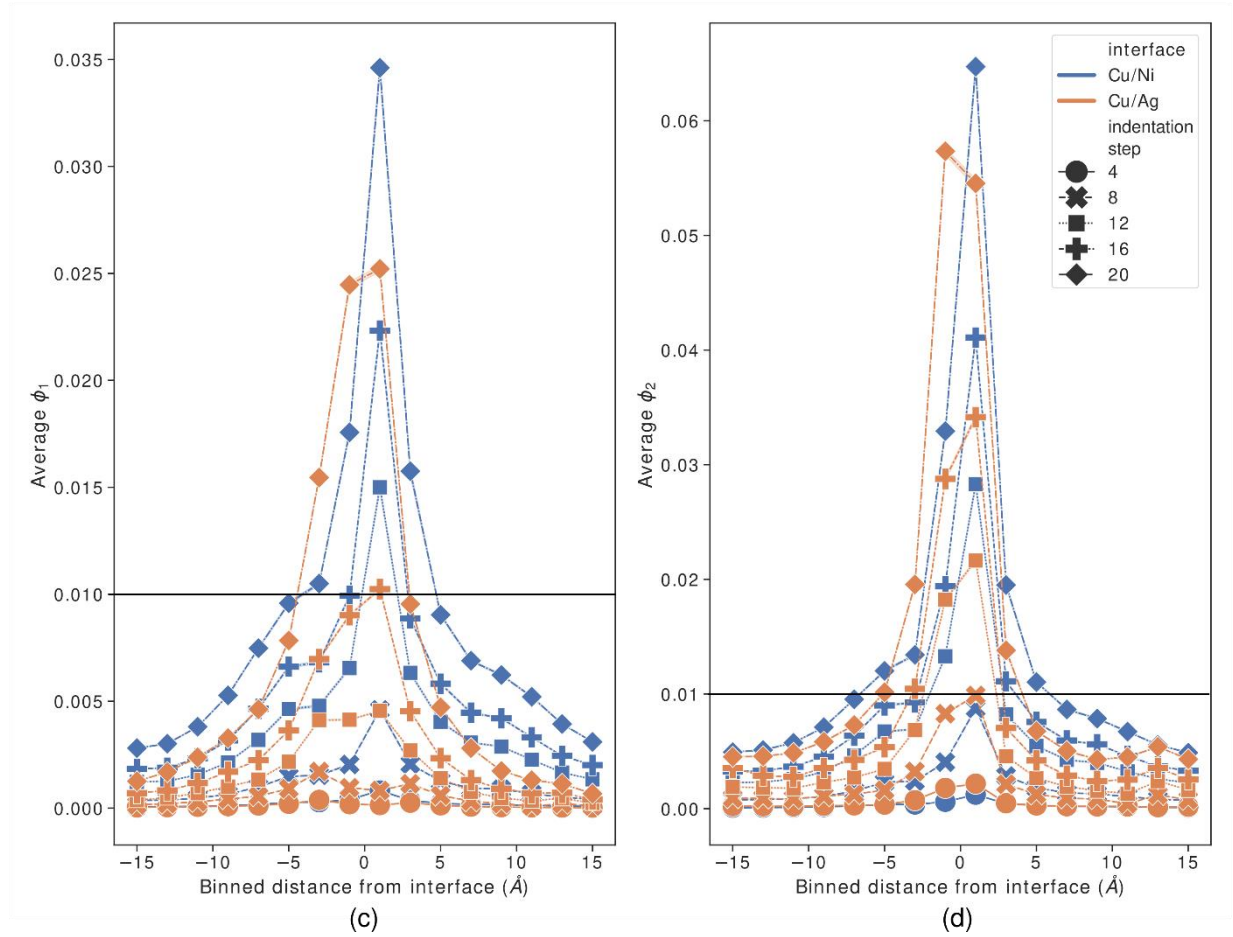
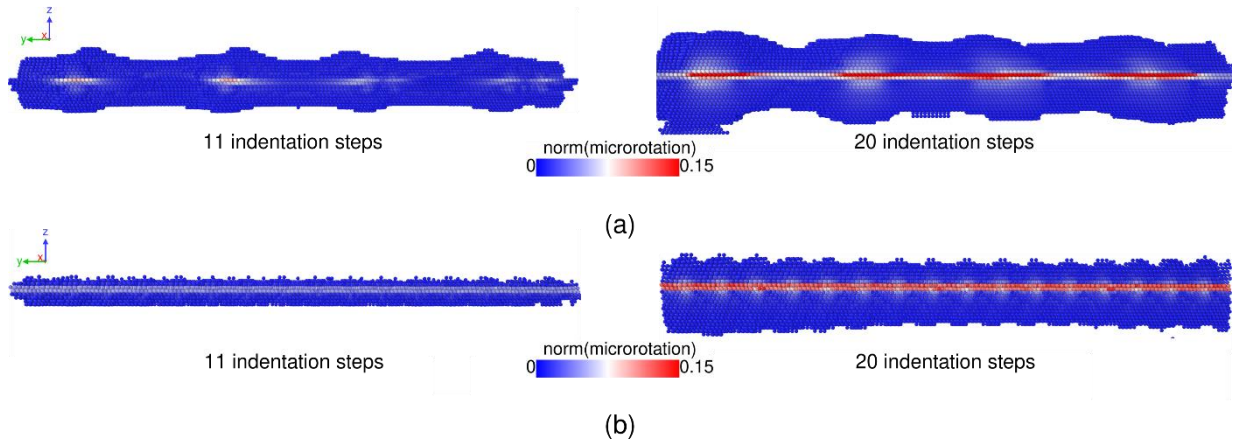


Figure 7: Cross section of interface with atoms colored by magnitude of the microrotation vector for a) Ni/Cu and b) Cu/Ag interfaces. Atoms with microrotation magnitudes less than 0.01 are hidden. The islands are much larger for Ni/Cu, implying deformation of lattice structure farther from interface, and in both cases extend primarily from misfit nodes. c) Cu/Ag and d) Ni/Cu average microrotation magnitudes for different components versus distance shows larger microrotation fields away from interface for Ni/Cu. The horizontal black lines at 0.01 microrotation emphasize regions of non-negligible microrotation.

1  
2  
3  
4 The depth of penetration of the deformation fields originating from misfit nodes may be a  
5 measure of the interface's ability to nucleate dislocations and transmit slip, both processes  
6 requiring extended restructuring of the atomic structure. Because dislocation nucleation  
7 requires participation of neighboring planes, interfaces which have larger deformation  
8 fields extending from misfit nodes likely have lower required critical stresses for  
9 dislocation nucleation. This analysis suggests that the smaller misfit node spacing in Cu/Ag  
10 corresponds to an increased stress required for dislocation nucleation from the interface.  
11 The effects of the observed complex deformation of the Ni/Cu interface misfit patterns on  
12 this critical stress for nucleation requires further study.  
13  
14  
15  
16  
17

## 18 Conclusions

19  
20 The evolution of interface structures in both Cu/Ag and Ni/Cu bilayers is studied in this  
21 article using the CAC methodology. The microrotation is calculated for every atom at the  
22 interface to quantify restructuring associated with the deformation of the interface misfit  
23 patterns. The primary findings of these studies are as follows:  
24

- 25 • Dislocation stress fields can cause increasing degrees of deformation to interface  
26 misfit structures in which non-uniform expansion/contraction occurs.
- 27 • Misfit nodes are seen to glide away from slip plane impingement sites in Ni/Cu. This is  
28 expected to cause further decreases in the interface blocking strength as compared to  
29 Cu/Ag, in which lattice dislocations are more likely to impinge upon misfit nodes.
- 30 • Deformation of the misfit patterns at the Cu/Ag interface occurs more uniformly along  
31 the interface due to the higher misfit density. For Ni/Cu the deformation is localized at  
32 the fewer nodes that are present resulting in higher maximum magnitudes of  
33 deformation. This is quantitatively observed using the microrotation as a metric.
- 34 • Misfit pattern evolution is accompanied by regions of restructuring in the phase  
35 interiors which extend from the misfit dislocation nodes. The depth of penetration for  
36 these regions is larger in Ni/Cu due to the larger degrees of restructuring localized to  
37 the misfit dislocation nodes.  
38  
39  
40  
41  
42

43 Future work will address various open questions. The extent to which the change in misfit  
44 pattern affects the interface blocking strength will be quantified. The degree to which the  
45 misfit node spacing impacts the slip transmission will be characterized through  
46 comparisons between Ni/Cu and Cu/Ag. The evolution of interface structure during  
47 sequential slip transmissions and associated changes in interface blocking strength will  
48 also be studied. The difference in Burgers vectors for both components in a bilayered  
49 material must be accommodated within the interface for slip transmission to occur which  
50 manifests as a step left on the interface. It is expected that the growth of this step will  
51 increase the interface blocking strength [45]. Increases to the blocking strength may result  
52 in a change in mechanism from slip transmission to a more favorable nucleation of  
53 dislocations from the step [46]. The increased stability of the Cu/Ag interface misfit  
54 structure and the lower misfit dislocation spacing, observed in this work, are expected to  
55 result in a higher blocking strength than that of Ni/Cu.  
56  
57  
58  
59  
60  
61  
62  
63  
64  
65



## Methodology

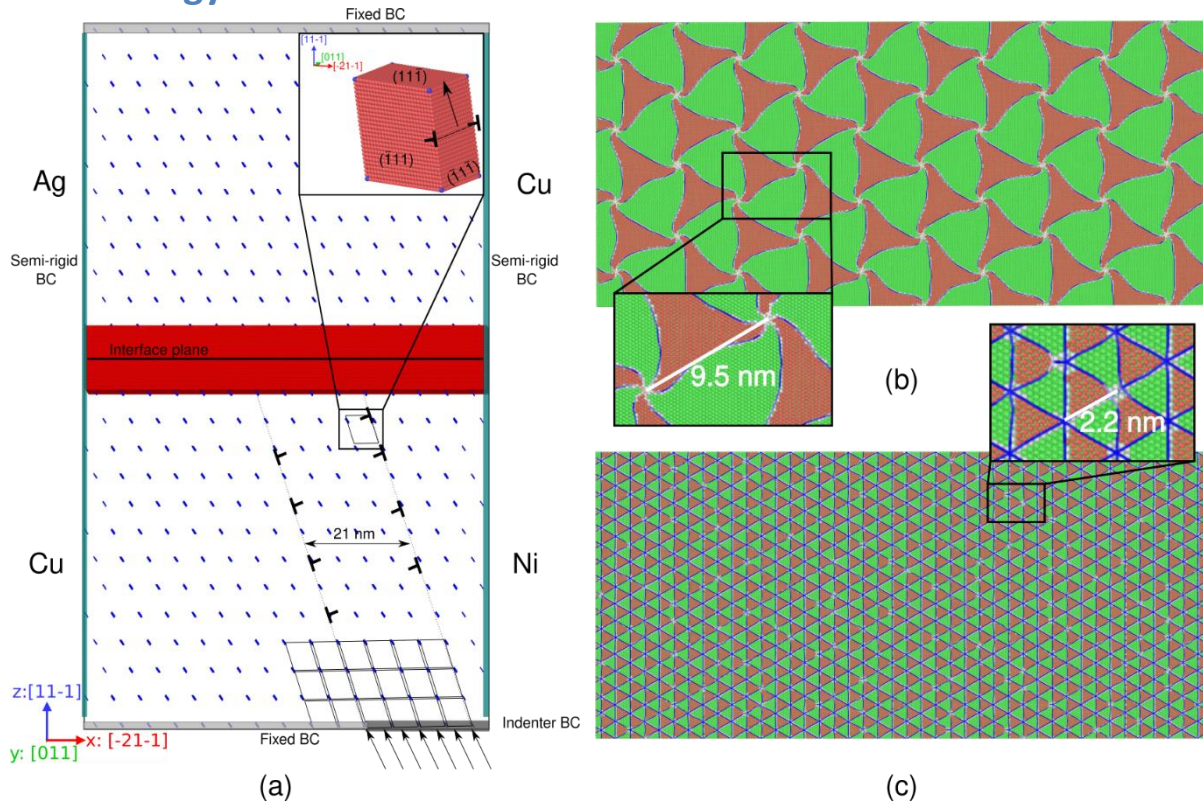


Figure 8: a) Atom (red) and finite element node (blue) representation of model with overlaid schematics of boundary conditions and CAC finite element shapes. b) Common neighbor analysis of relaxed Ni/Cu interface and c) common neighbor analysis of relaxed Cu/Ag interface. Green atoms are FCC, red atoms are HCP, blue atoms are BCC, and gray atoms are others. Insets represent zoomed in sections of interfaces capturing misfit nodes. Misfit node spacings of 9.5 nm and 2.2 nm agree with values from the literature [21].

Figure 8 presents a schematic of the model under investigation. These bicrystal models are partitioned into two coarse-grained regions for the bulk crystals and one atomistic region which contains the semi-coherent interface. The coarse-grained regions reduce the number of degrees of freedom while allowing for the transmission of dislocations from the surface of the model to the interface. This is very important in reducing computational time for periodic energy minimization. To ensure that the dislocations are represented correctly in the coarse-grained domain, 3D rhombohedral elements are used that utilize a second nearest neighbor interpolation scheme and have all faces aligned to  $\{111\}$  slip planes [30]. Each element in the coarse-grained domain represents 15,625 atoms. Bicrystal models comprised of alternating Cu and Ni layers or Cu and Ag layers are studied, each containing one semi-coherent  $(11\bar{1})$  interface. These models are generated by stacking two regions of either Cu and Ni or Cu and Ag in the  $z$  direction and then performing energy minimization

1  
2  
3  
4 using the fast inertial relaxation engine (FIRE) [47]. Calculated misfit node spacings are 9.5  
5 nm for the Ni/Cu interface and 2.2 nm for the Cu/Ag which agree well with computational  
6 studies found in the literature [21]. Additionally, dislocations entering misfit nodes are  
7 seen to form a spiral pattern characteristic of Ni/Cu [19] but not observed for undeformed  
8 Cu/Ag interfaces [21]. The misfit dislocation densities for the relaxed interfaces are  
9 0.39028 and 1.5673 nm<sup>-1</sup> for Ni/Cu and Cu/Ag respectively.  
10  
11

12 To determine the minimum number of atomic layers between the interface and coarse-  
13 grained regions needed to fully capture relevant interface reconstructive reactions, a mesh  
14 sensitivity study is conducted on the Ni/Cu semi-coherent interface. The trilinear shape  
15 function used in the finite elements within the coarse-grained domains does not accurately  
16 capture these non-linear displacement fields, inhibiting the correct development of the  
17 interface misfit structure. Therefore, it is critically important to quantify the minimum  
18 distance from interface to coarse-grained region to ensure correct modeling of interface  
19 evolution. Models containing an unrelaxed semi-coherent Ni/Cu interface with different  
20 numbers of atomic layers at the interface were energy minimized. We built a reference  
21 model with 20 atomic layers extending from the interface as further increases in the  
22 number of atomic layers yielded fewer benefits to accuracy. A fully atomistic reference  
23 model was not used due to the simulation cell sizes, which would require approximately 40  
24 million atoms. Each test model was compared to the reference model as follows. First,  
25 atoms within 2 nm of the interface on either side in the test model were mapped to the  
26 nearest atom in the reference model. Then, the error metric is computed as the distance  
27 between an atom at the interface and its nearest counterpart in the reference model. The  
28 model schematic and results of this sensitivity study are shown in Figure 9. Convergence in  
29 the error based on comparison with the most highly refined solution occurs for models  
30 having more than approximately 16 atomic layers; accordingly, the models are constructed  
31 with 16 atomic layers on each side of the interface. This is equivalent to an atomic layer  
32 thickness of 5 nm from the interface to the coarse-grained region. This is larger than the  
33 minimum thicknesses of 1.2 nm required for strontium-titanate grain boundaries [48], and  
34 larger than those used in some previous CAC simulations of approximately 2.2 nm [35] and  
35 3.5 nm [33, 34] thickness from the interface to the coarse-grained region. This difference  
36 likely results from the highly mobile misfit dislocations within the bimetal interfaces that  
37 require large displacements to form the spiral misfit pattern that are not present in the  
38 previously discussed interfaces. The small amounts of uniformly distributed error at higher  
39 numbers of atomic layers results from uniform shifts in interface position across periodic  
40 boundaries. This minimum number of atomic layers is also used for the Cu/Ag model, as  
41 the minimization of the Cu/Ag interface is accompanied by much smaller changes to the  
42 misfit dislocation structure than in the Ni/Cu interface.  
43  
44  
45  
46  
47  
48  
49  
50  
51  
52  
53  
54  
55  
56  
57  
58  
59  
60  
61  
62  
63  
64  
65

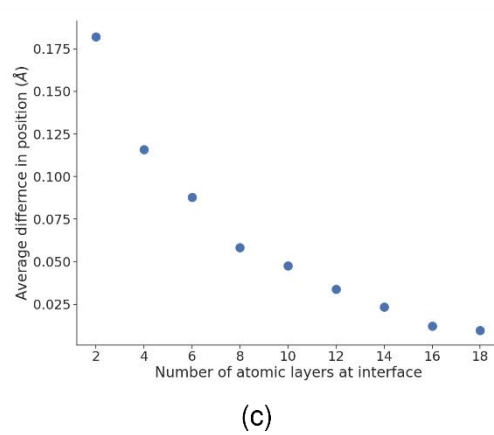
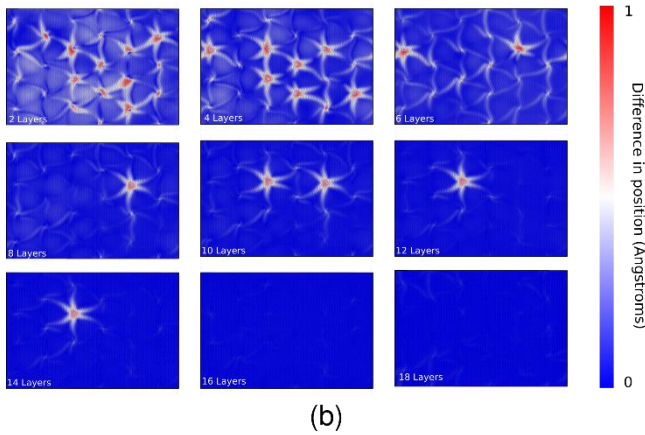
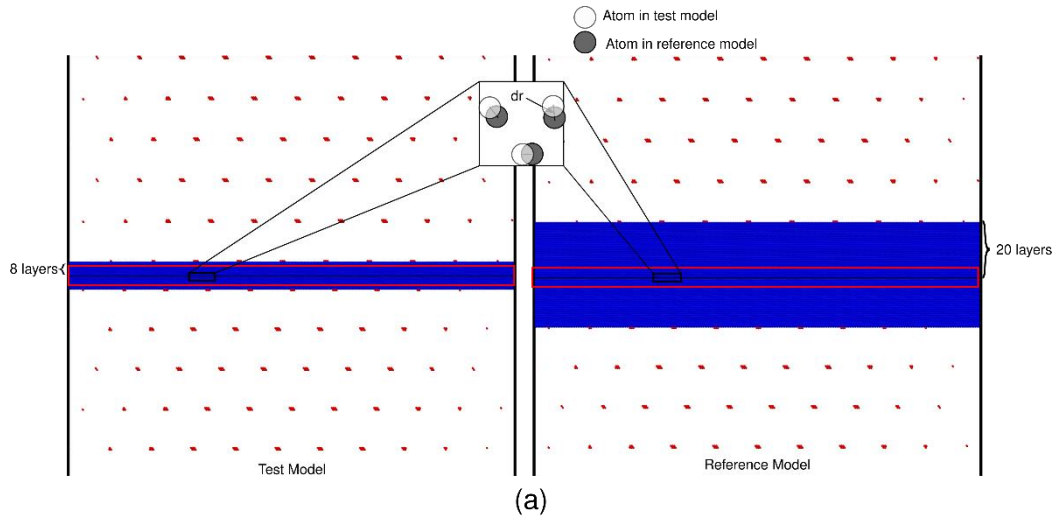


Figure 9: a) Schematic of mesh sensitivity models showing calculation of “ $dr$ ” which is the difference in atom position between an atom in the test model and the atom in the reference model. b) Local error maps of the interface show error in the minimization of the Ni/Cu interface primarily associated with interface nodes which have high degrees of restructuring. c) The error plot shows that convergence of atomic positions is reached at approximately 16 atomic layers.

As shown in Figure 8, the orientations for the model are  $x=[\bar{2}11]$ ,  $y=[011]$ ,  $z=[11\bar{1}]$ . Periodic boundaries are enforced in the  $x$  and  $y$  directions and care is taken when setting model dimensions in order to ensure that periodicity of the interface structure and the bulk layers is maintained. The model has dimensions of  $x \approx 82.35$  nm,  $y \approx 38.34$  nm, and  $z \approx 69.00$  nm corresponding to a layer thickness of 34.5 nm for the Ni/Cu model. The Cu/Ag model has dimensions of  $x \approx 80.15$  nm,  $y \approx 37.59$  nm, and  $z \approx 74.52$  nm corresponding to a layer thickness of approximately 37.3 nm. To generate dislocations on specific intersecting slip planes, elements and atoms within a rectangular region at the bottom surface are effectively indented along interelement discontinuities generating  $60^\circ$  mixed character dislocations on distinct slip planes that are offset by approximately 21 nm. This is done by prescribing a displacement to the portion of atoms and nodes with  $x$  positions between 38

1  
2  
3  
4 and 59 nm at the bottom surface and keeping all other atoms and nodes at the surface  
5 fixed. This simple approach to imposing indentation is satisfactory for the purpose of  
6 generating distinct dislocations to study the evolution of interface structure as a result of  
7 dislocation stress fields [30]. For both models, indentation is performed on the bulk  
8 material which has the smaller lattice constant, i.e. Ni in the Ni/Cu system and Cu in the  
9 Cu/Ag system, such that lattice dislocations are under tensile coherency stresses from the  
10 interface. This is to compare the lattice dislocation induced misfit dislocation evolution for  
11 different misfit dislocation node spacings under similar stress states. Future studies will  
12 investigate whether the interaction of dislocation stress fields with the interface coherency  
13 stress fields of the originating bulk material, the sign of which depends on whether the bulk  
14 material has the larger or smaller lattice constant, causes differing interface misfit  
15 dislocation structure evolution that contributes to the direction-dependent slip  
16 transmission blocking strength observed in the literature [12, 49].  
17  
18  
19  
20  
21

22 Dislocations are generated on intersecting  $(\bar{1}11)$  slip planes. Other more complex methods  
23 for simulating indentation exist for predicting hardness from atomistic simulations [50,  
24 51]. The displacement magnitude at every indentation step is 0.3 Å. Three 60° mixed  
25 character dislocations are generated per plane with a max indentation step of 6.6 Å. A small  
26 degree of asymmetry is noted in the progression of dislocations on both slip planes.  
27 Dislocations are found to progress first along the slip plane which impinges on the interface  
28 closer to the center of the model. This small asymmetry likely arises from the difference in  
29 the proximity of each slip plane to the semi-rigid boundaries, which may impart additional  
30 stresses that hinder the motion of the dislocations. After every indentation step, quenched  
31 dynamics [52] is run for 10 ps, or 1000 timesteps, and then energy minimization is  
32 performed using FIRE. This approach better approximates the sequence of constrained  
33 equilibrium states pertaining to quasistatic deformation under the imposed boundary  
34 conditions; simple quasi-static energy minimization, in contrast, can fall into local energy  
35 minima in complex energy landscapes. During indentation, semi-rigid boundaries are used  
36 for atoms at the boundaries of the cell in the x direction and periodic dimensions are used  
37 in the y, or lattice dislocation line, direction. To create a rectangular domain, atoms are  
38 used to fill the jagged interstices between coarse-grained elements along all dimensions. **To**  
39 **ensure that the indenter distance did not have a significant impact on the interface**  
40 **structures observed, two models with indenter distances of 34.5 nm and 65 nm from the**  
41 **interface were investigated. Figure 10 shows the interface structure at the indentation step**  
42 **prior to the dislocation entering the interface. The interface misfit structures in both cases**  
43 **are similar. Analysis of the node distribution along the x direction also matches in both**  
44 **cases with an increased misfit node distance from the slip plane impingement for the larger**  
45 **model resulting from the increased shear stress induced by additional dislocations in the**  
46 **pileup. The 34.5 nm model was therefore considered to have sufficient separation between**  
47 **indenter and interface for comparing the evolution of misfit patterns for Ni/Cu and Cu/Ag.**  
48  
49  
50  
51  
52  
53  
54  
55  
56  
57  
58  
59  
60  
61  
62  
63  
64  
65

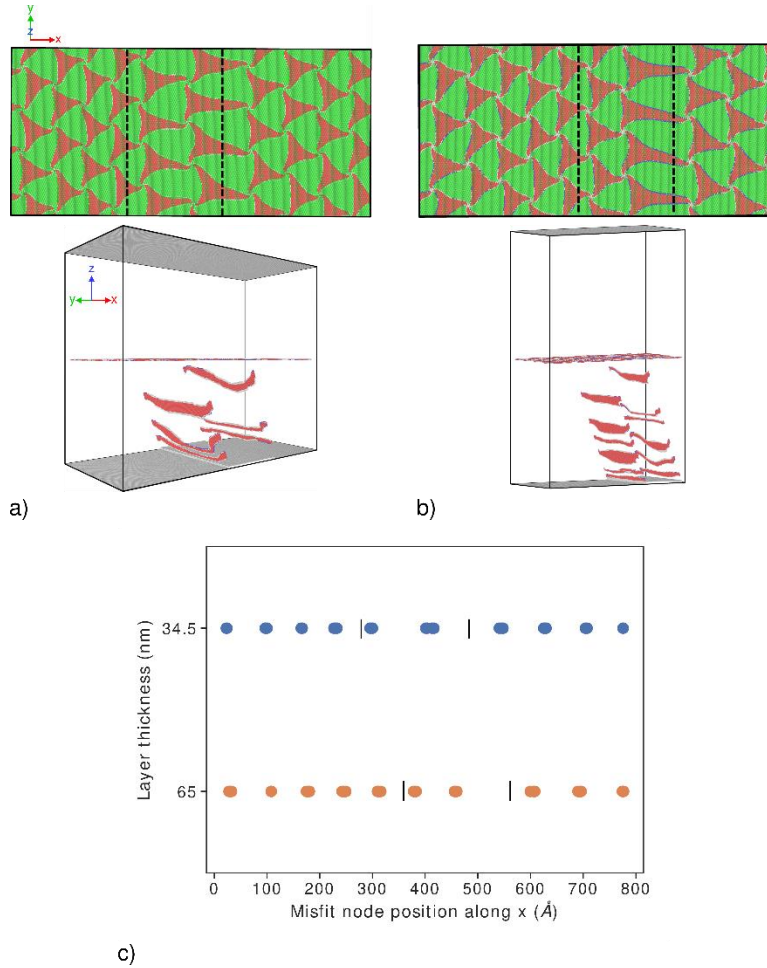


Figure 10: a) Interface and dislocation structure for the 34.5 nm layer thickness model and b) 65 nm layer thickness model at the timestep prior to the lattice dislocation entering the interface. c) Shows the misfit node positions along the x direction with black lines denoting the slip plane impingement sites. Similar structures are seen in both models with increased distance of misfit nodes from the impingement sites in the 65 nm model resulting from the additional shear stress imparted by the long-range fields of the additional dislocations in the pileup.

The only pertinent constitutive law for both the coarse-grained region and the atomistic region is the interatomic potential. For the Ni/Cu models the interatomic potential developed by Onat and Durukanoğlu is used [53] which accurately captures the stacking fault energies for each individual component and captures the alloy structure energetics accurately. The Williams, Mishin, and Hamilton [54] potential for Cu/Ag is used, which accurately captures the energetics of both bulk and cross-interaction terms. Accordingly, the equilibrium lattice constants are 3.615, 4.09, and 3.52 Å for Cu, Ag, and Ni, respectively. All simulations are run using the PyCAC code [55]. To visualize the models, coarse-grained regions are converted to the equivalent atomistic model and OVITO [56] is used. The Dislocation Extraction Algorithm (DXA) [57] is used for visualizing dislocations. Common neighbor analysis (CNA) [58] is used for the visualization of atomic structures and qualitative comparisons. In so doing, a variety of continuum metrics can be computed

1  
2  
3  
4 based on relative motion of local neighborhood of each atom to promote enhanced  
5 understanding of the structural evolution. In particular, the microrotation is an informative  
6 metric to quantify in more detail the interface reconstruction [44] and is defined by the  
7 vector:  
8  
9

$$\phi_k = -\frac{1}{2} \varepsilon_{ijk} (R_{skew})_{ij} \quad (1)$$

10  
11  
12  
13  
14  
15  
16  
17 where  $\varepsilon$  is the permutation symbol and  $R_{skew}$  is the skew symmetric part of the rotation  
18 tensor in the polar decomposition of the deformation gradient, i.e.,  
19

$$\mathbf{F} = \mathbf{R}\mathbf{U} \quad (2)$$

$$R_{skew} = \frac{1}{2}(\mathbf{R} - \mathbf{R}^T) \quad (3)$$

20  
21  
22  
23  
24  
25  
26  
27 Here,  $\mathbf{R}$  is the rotation,  $\mathbf{U}$  is the right stretch tensor, and  $\mathbf{F}$  is the deformation gradient,  
28 computed within some finite radius of each atom containing only first nearest neighbors.  
29 To calculate the rotation tensor, first the deformation gradient  $\mathbf{F}$  is calculated from the  
30 current and reference atomic configurations. The right stretch tensor  $\mathbf{U}$  is then computed  
31 using:  
32

$$\mathbf{U} = \sqrt{\mathbf{F}^T \mathbf{F}} \quad (4)$$

33  
34  
35  
36 The rotation tensor can then be computed from  $\mathbf{F}$  and the inverse of  $\mathbf{U}$ . More in-depth  
37 descriptions on the calculation of the deformation gradient and microrotation for  
38 atomistics can be found in [59,60].  
39  
40

## 41 42 Acknowledgements

43  
44  
45 This work is based on research supported by the National Science Foundation under the  
46 grants CMMI-1761553 and CMMI-1761512. All presented simulations were conducted  
47 using XSEDE resources under allocation TG-MSS150010.  
48  
49

## 50 51 References

- 52  
53 [1] X. Wu, P. Jiang, L. Chen, F. Yuan, and Y. T. Zhu: Extraordinary strain hardening by gradient  
54 structure. *Proceedings of the National Academy of Sciences*.111(20), 7197–7201 (2014).  
55  
56 [2] X. Wu, M. Yang, F. Yuan, G. Wu, Y. Wei, X. Huang, and Y. Zhu: Heterogeneous lamella struc-  
57 ture unites ultrafine-grain strength with coarse-grain ductility. *Proceedings of the Na-*  
58 *tional Academy of Sciences*.112(47), 14501–14505 (2015).  
59  
60  
61  
62  
63  
64  
65

- 1  
2  
3  
4 [3] J. Moering, X. Ma, G. Chen, P. Miao, G. Li, G. Qian, S. Mathaudhu, and Y. Zhu: The role of shear  
5 strain on texture and microstructural gradients in low carbon steel processed by surface  
6 mechanical attrition treatment. *Scripta Materialia*.108, 100–103 (2015).  
7  
8 [4] A. Misra: 7 - mechanical behavior of metallic nanolaminates, in *Nanostructure control of*  
9 *materials*, R. H. J. Hannink and A. J. Hill, Eds. Woodhead Publishing, 2006, 146–176.  
10  
11 [5] N. A. Mara and I. J. Beyerlein: Interface-dominant multilayers fabricated by severe plastic  
12 deformation: Stability under extreme conditions. *Current Opinion in Solid State and Mate-*  
13 *rials Science*.19(5), 265–276 (2015).  
14  
15 [6] C. C. Tasan, M. Diehl, D. Yan, M. Bechtold, F. Roters, L. Schemmann, C. Zheng, N. Peranio, D.  
16 Ponge, M. Koyama, and others: An overview of dual-phase steels: Advances in micro-  
17 structureoriented processing and micromechanically guided design. *Annual Review of*  
18 *Materials Research*.45, 391–431 (2015).  
19  
20 [7] A. Sáenz-Trevizo and A. M. Hodge: Nanomaterials by design: A review of nanoscale metallic  
21 multilayers. *Nanotechnology*.31(29), 292002 (2020).  
22  
23 [8] B. M. Clemens, H. Kung, and S. A. Barnett: Structure and Strength of Multilayers. *MRS*  
24 *Bulletin*.24(2), 20–26 (1999).  
25  
26 [9] Q. Zhou, J. Y. Xie, F. Wang, P. Huang, K. W. Xu, and T. J. Lu: The mechanical behavior of  
27 nanoscale metallic multilayers: A survey. *Acta Mechanica Sinica*.31(3), 319–337 (2015).  
28  
29 [10] R. G. Hoagland, R. J. Kurtz, and C. H. Henager: Slip resistance of interfaces and the strength  
30 of metallic multilayer composites. *Scripta Materialia*.50(6), 775–779 (2004).  
31  
32 [11] I. N. Mastorakos, H. M. Zbib, and D. F. Bahr: Deformation mechanisms and strength in  
33 nanoscale multilayer metallic composites with coherent and incoherent interfaces. *Ap-*  
34 *plied Physics Letters*.94(17), 173114 (2009).  
35  
36 [12] M. Xiang, Y. Liao, K. Wang, G. Lu, and J. Chen: Shock-induced plasticity in semi-coherent  
37 {111} cu-ni multilayers. *International Journal of Plasticity*.103, 23–38 (2018).  
38  
39 [13] S. Shao, J. Wang, I. J. Beyerlein, and A. Misra: Glide dislocation nucleation from dislocation  
40 nodes at semi-coherent {1 1 1} Cu–Ni interfaces. *Acta Materialia*.98, 206–220 (2015).  
41  
42 [14] X. Y. Chen, X. F. Kong, A. Misra, D. Legut, B. N. Yao, T. C. Germann, and R. F. Zhang: Effect of  
43 dynamic evolution of misfit dislocation pattern on dislocation nucleation and shear slid-  
44 ing at semi-coherent bimetal interfaces. *Acta Materialia*.143, 107–120 (2018).  
45  
46 [15] H. Yang, L. Zhu, R. Zhang, J. Zhou, and Z. Sun: Influence of high stacking-fault energy on the  
47 dissociation mechanisms of misfit dislocations at semi-coherent interfaces. *International*  
48 *Journal of Plasticity*.126, 102610 (2020).  
49  
50 [16] R. F. Zhang, T. C. Germann, X. Y. Liu, J. Wang, and I. J. Beyerlein: Layer size effect on the  
51 shock compression behavior of fcc–bcc nanolaminates. *Acta Materialia*.79, 74–83 (2014).  
52  
53  
54  
55  
56  
57  
58  
59  
60  
61  
62  
63  
64  
65

- 1  
2  
3  
4 [17] R. Dikken and M. Khajeh Salehani: Edge dislocation impingement on interfaces between  
5 dissimilar metals, 2017.  
6  
7 [18] A. Couret, J. Crestou, S. Farenc, G. Molenat, N. Clement, A. Coujou, and D. Caillard: In situ  
8 deformation in T.E.M.: Recent developments. *Microscopy Microanalysis Microstruc-*  
9 *tures*.4(2– 3), 153–170 (1993).  
10  
11 [19] S. Shao, J. Wang, A. Misra, and R. G. Hoagland: Spiral patterns of dislocations at nodes in  
12 (111) semi-coherent FCC interfaces. *Scientific Reports*.3(1), (2013).  
13  
14 [20] H. Yang, L. Zhu, R. Zhang, J. Zhou, and Z. Sun: Shearing dominated by the coupling of the  
15 interfacial misfit and atomic bonding at the FCC (111) semi-coherent interfaces. *Materi-*  
16 *als & Design*.186, 108294 (2020).  
17  
18 [21] S. Shao, J. Wang, and A. Misra: Energy minimization mechanisms of semi-coherent interfac-  
19 es. *Journal of Applied Physics*.116(2), 023508 (2014).  
20  
21 [22] E. B. Tadmor, M. Ortiz, and R. Phillips: Quasicontinuum analysis of defects in solids. *Philo-*  
22 *sophical Magazine A*.73(6), 1529–1563 (1996).  
23  
24 [23] E. B. Tadmor, F. Legoll, W. K. Kim, L. M. Dupuy, and R. E. Miller: Finite-temperature quasi-  
25 continuum. *Applied Mechanics Reviews*.65(1), (2013).  
26  
27 [24] L. E. Shilkrot, R. E. Miller, and W. A. Curtin: Coupled atomistic and discrete dislocation  
28 plasticity. *Physical Review Letters*.89(2), (2002).  
29  
30 [25] G. Ancaux, T. Junge, M. Hodapp, J. Cho, J.-F. Molinari, and W. A. Curtin: The coupled atomis-  
31 tic/discrete-dislocation method in 3d part I: Concept and algorithms. *Journal of the Me-*  
32 *chanics and Physics of Solids*.118, 152–171 (2018).  
33  
34 [26] D. L. McDowell: Multiscale modeling of interfaces, dislocations, and dislocation field  
35 plasticity, in *Mesoscale models*, Springer International Publishing, 2018, 195–297.  
36  
37 [27] M. Dewald and W. A. Curtin: Analysis and minimization of dislocation interactions with  
38 atomistic/continuum interfaces. *Modelling and Simulation in Materials Science and Engi-*  
39 *neering*.14(3), 497–514 (2006).  
40  
41 [28] T. Shimokawa, T. Kinari, and S. Shintaku: Interaction mechanism between edge dislocations  
42 and asymmetrical tilt grain boundaries investigated via quasicontinuum simulations.  
43 *Physical Review B*.75(14), (2007).  
44  
45 [29] Y. Chen, S. Shabanov, and D. L. McDowell: Concurrent atomistic-continuum modeling of  
46 crystalline materials. *Journal of Applied Physics*.126(10), 101101 (2019).  
47  
48 [30] S. Xu, R. Che, L. Xiong, Y. Chen, and D. L. McDowell: A quasistatic implementation of the  
49 concurrent atomistic-continuum method for FCC crystals. *International Journal of Plasti-*  
50 *city*.72, 91–126 (2015).  
51  
52 [31] S. Xu, D. L. McDowell, and I. J. Beyerlein: Sequential obstacle interactions with dislocations  
53 in a planar array. *Acta Materialia*.174, 160–172 (2019).  
54  
55  
56  
57  
58  
59  
60  
61  
62  
63  
64  
65

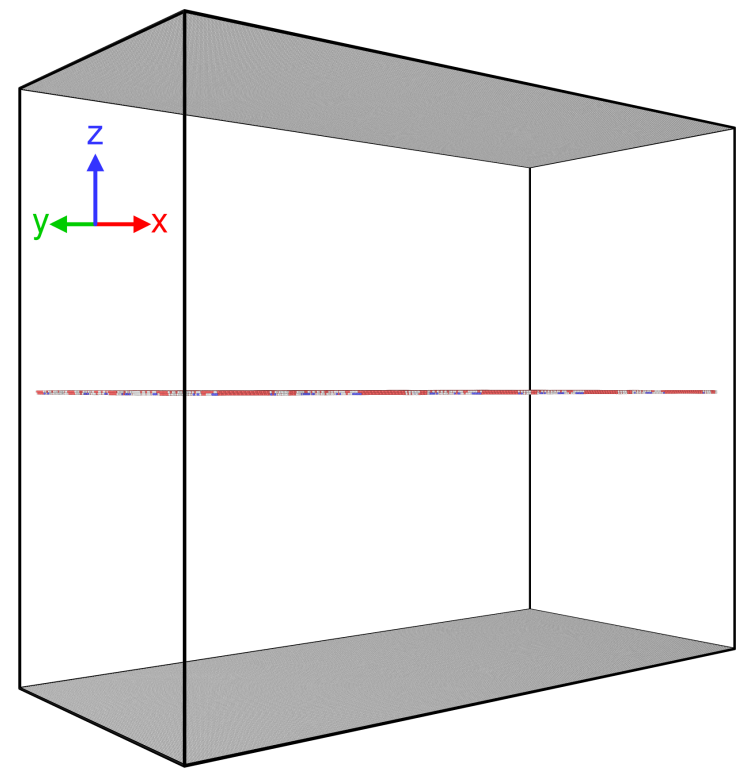
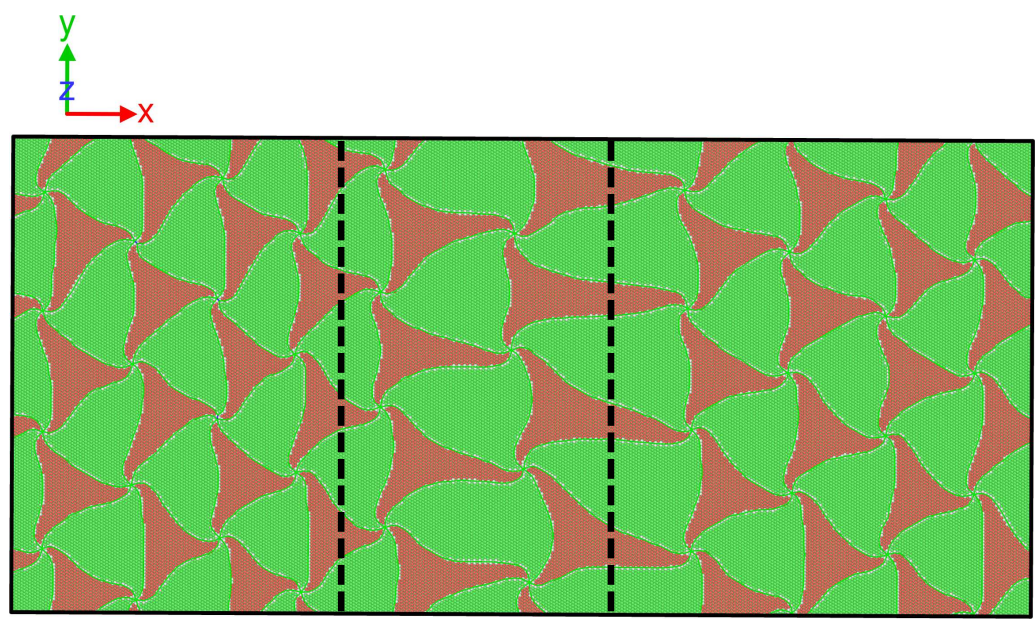
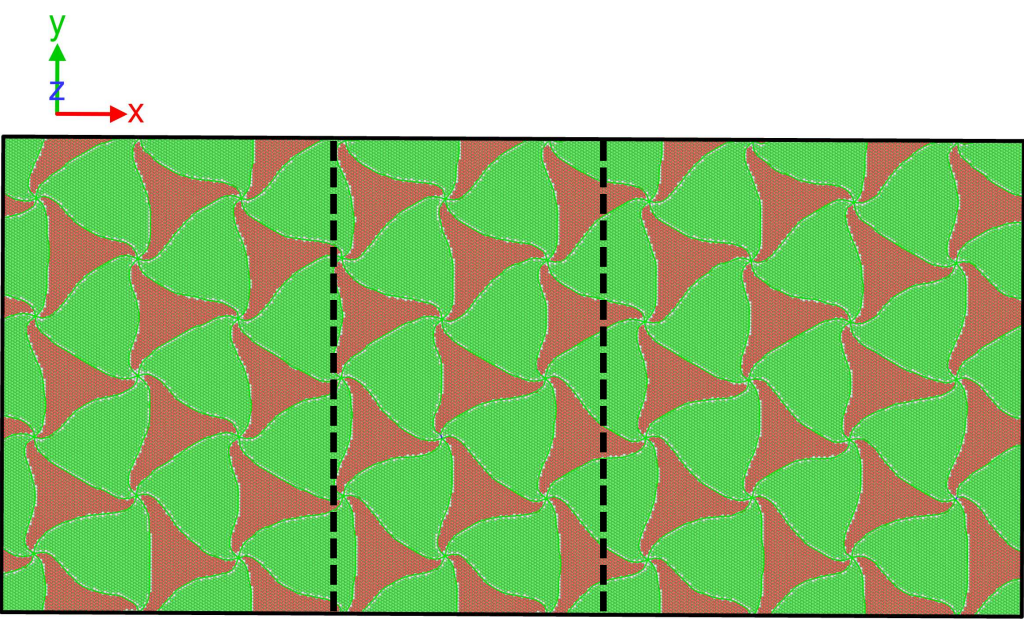


- 1  
2  
3  
4 [32] L. Xiong, D. L. McDowell, and Y. Chen: Nucleation and growth of dislocation loops in Cu, Al  
5 and Si by a concurrent atomistic-continuum method. *Scripta Materialia*.67(7–8), 633–636  
6 (2012).  
7  
8 [33] S. Xu, L. Xiong, Y. Chen, and D. L. McDowell: Sequential slip transfer of mixed-character  
9 dislocations across  $\Sigma 3$  coherent twin boundary in FCC metals: A concurrent atomistic-  
10 continuum study. *npj Computational Materials*.2(1), 15016 (2016).  
11  
12 [34] S. Xu, L. Xiong, Y. Chen, and D. L. McDowell: Comparing EAM potentials to model slip  
13 transfer of sequential mixed character dislocations across two symmetric tilt grain  
14 boundaries in Ni. *JOM*.69(5), 814–821 (2017).  
15  
16 [35] S. Xu, Y. Li, and Y. Chen: Si/Ge (111) semicoherent interfaces: Responses to an in-plane  
17 shear and interactions with lattice dislocations. *physica status solidi (b)*.257, 2000274  
18 (2020).  
19  
20 [36] Y. Li, Z. Fan, W. Li, D. L. McDowell, and Y. Chen: A multiscale study of misfit dislocations in  
21 PbTe/PbSe(001) heteroepitaxy. *Journal of Materials Research*.34(13), 2306–2314 (2019).  
22  
23 [37] H. Chen, S. Xu, W. Li, R. Ji, T. Phan, and L. Xiong: A spatial decomposition parallel algorithm  
24 for a concurrent atomistic-continuum simulator and its preliminary applications. *Compu-  
25 tational Materials Science*.144, 1–10 (2018).  
26  
27 [38] W.-R. Jian, M. Zhang, S. Xu, and I. J. Beyerlein: Atomistic simulations of dynamics of an edge  
28 dislocation and its interaction with a void in copper: A comparative study. *Modelling and  
29 Simulation in Materials Science and Engineering*.28(4), 045004 (2020).  
30  
31 [39] G. H. Vineyard: Frequency factors and isotope effects in solid state rate processes. *Journal of  
32 Physics and Chemistry of Solids*.3(1–2), 121–127 (1957).  
33  
34 [40] A. F. Voter and J. D. Doll: Transition state theory description of surface self-diffusion:  
35 Comparison with classical trajectory results. *The Journal of Chemical Physics*.80(11),  
36 5832– 5838 (1984).  
37  
38 [41] S. Ryu, K. Kang, and W. Cai: Predicting the dislocation nucleation rate as a function of  
39 temperature and stress. *Journal of Materials Research*.26(18), 2335–2354 (2011).  
40  
41 [42] G. Henkelman, B. P. Uberuaga, and H. Jónsson: A climbing image nudged elastic band  
42 method for finding saddle points and minimum energy paths. *The Journal of Chemical  
43 Physics*.113(22), 9901–9904 (2000).  
44  
45 [43] X. Zhang, B. Zhang, Y. Mu, S. Shao, C. D. Wick, B. R. Ramachandran, and W. J. Meng: Me-  
46 chanical failure of metal/ceramic interfacial regions under shear loading. *Acta  
47 Materialia*.138, 224–236 (2017).  
48  
49 [44] G. J. Tucker, J. A. Zimmerman, and D. L. McDowell: Continuum metrics for deformation and  
50 microrotation from atomistic simulations: Application to grain boundaries. *International  
51 Journal of Engineering Science*.49(12), 1424–1434 (2011).  
52  
53  
54  
55  
56  
57  
58  
59  
60  
61  
62  
63  
64  
65

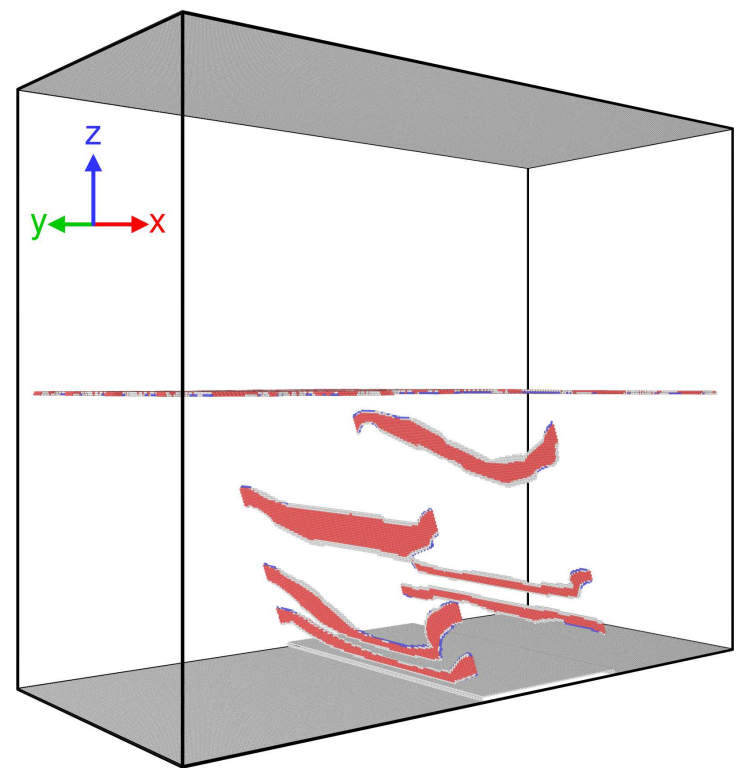
- 1  
2  
3  
4 [45] J. Wang: Atomistic simulations of dislocation pileup: Grain boundaries interaction.  
5 *JOM*.67(7), 1515–1525 (2015).  
6  
7 [46] M. Dodaran, J. Wang, Y. Chen, W. J. Meng, and S. Shao: Energetic, structural and mechanical  
8 properties of terraced interfaces. *Acta Materialia*.171, 92–107 (2019).  
9  
10 [47] E. Bitzek, P. Koskinen, F. Gähler, M. Moseler, and P. Gumbsch: Structural Relaxation Made  
11 Simple. *Physical Review Letters*.97(17), 170201 (2006).  
12  
13 [48] S. Yang and Y. Chen: Concurrent atomistic and continuum simulation of bi-crystal stronti-  
14 um titanate with tilt grain boundary. *Proceedings of the Royal Society A: Mathematical,*  
15 *Physical and Engineering Sciences*.471(2175), 20140758 (2015).  
16  
17 [49] X. Tian, J. Cui, M. Yang, K. Ma, and M. Xiang: Molecular dynamics simulations on shock  
18 response and spalling behaviors of semi-coherent {111} Cu-Al multilayers. *International*  
19 *Journal of Mechanical Sciences*.172, 105414 (2020).  
20  
21 [50] C. Ruestes, I. Alhafez, H. Urbassek, C. J. Ruestes, I. A. Alhafez, and H. M. Urbassek: Atomistic  
22 Studies of Nanoindentation— A Review of Recent Advances. *Crystals*.7(10), 293 (2017).  
23  
24 [51] S. Z. Chavoshi and S. Xu: Nanoindentation/scratching at finite temperatures: Insights from  
25 atomistic-based modeling. *Progress in Materials Science*.100, 1–20 (2019).  
26  
27 [52] E. Tadmor: *Modeling materials : Continuum, atomistic, and multiscale techniques*. Cambridge  
28 New York: Cambridge University Press, 2011.  
29  
30 [53] B. Onat and S. Durukanoglu: An optimized interatomic potential for Cu-Ni alloys with the  
31 embedded-atom method. *Journal of Physics Condensed Matter*.26(3), (2014).  
32  
33 [54] P. L. Williams, Y. Mishin, and J. C. Hamilton: An embedded-atom potential for the Cu-Ag  
34 system. *Modelling and Simulation in Materials Science and Engineering*.14(5), 817–833  
35 (2006).  
36  
37 [55] S. Xu, T. G. Payne, H. Chen, Y. Liu, L. Xiong, Y. Chen, and D. L. McDowell: PyCAC: The concur-  
38 rent atomistic-continuum simulation environment. *Journal of Materials Research*.33(7),  
39 857 (2018).  
40  
41 [56] A. Stukowski: Visualization and analysis of atomistic simulation data with OVITO—the open  
42 visualization tool. *Modelling and Simulation in Materials Science and Engineering*.18(1),  
43 015012 (2009).  
44  
45 [57] A. Stukowski and K. Albe: Dislocation detection algorithm for atomistic simulations.  
46 *Modelling and Simulation in Materials Science and Engineering*.18(2), 025016 (2010).  
47  
48 [58] D. Faken and H. Jónsson: Systematic analysis of local atomic structure combined with 3D  
49 computer graphics. *Computational Materials Science*.2(2), 279–286 (1994).  
50  
51 [59] J. A. Zimmerman, D. J. Bammann, and H. Gao: Deformation gradients for continuum me-  
52 chanical analysis of atomistic simulations. *International Journal of Solids and Struc-*  
53 *tures*.46(2), 238–253 (2009).  
54  
55  
56  
57  
58  
59  
60  
61  
62  
63  
64  
65

1  
2  
3  
4  
5  
6  
7  
8  
9  
10  
11  
12  
13  
14  
15  
16  
17  
18  
19  
20  
21  
22  
23  
24  
25  
26  
27  
28  
29  
30  
31  
32  
33  
34  
35  
36  
37  
38  
39  
40  
41  
42  
43  
44  
45  
46  
47  
48  
49  
50  
51  
52  
53  
54  
55  
56  
57  
58  
59  
60  
61  
62  
63  
64  
65

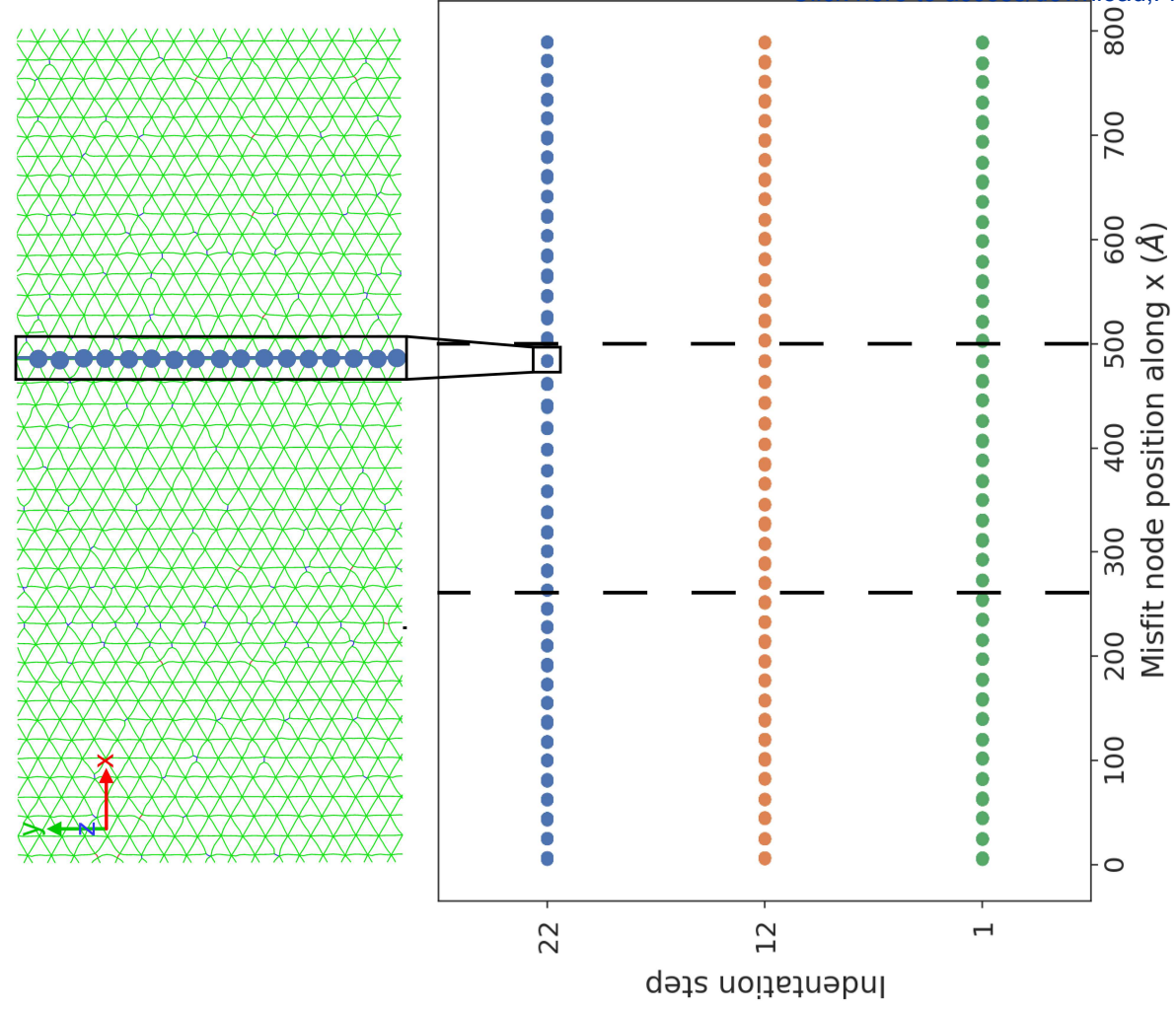
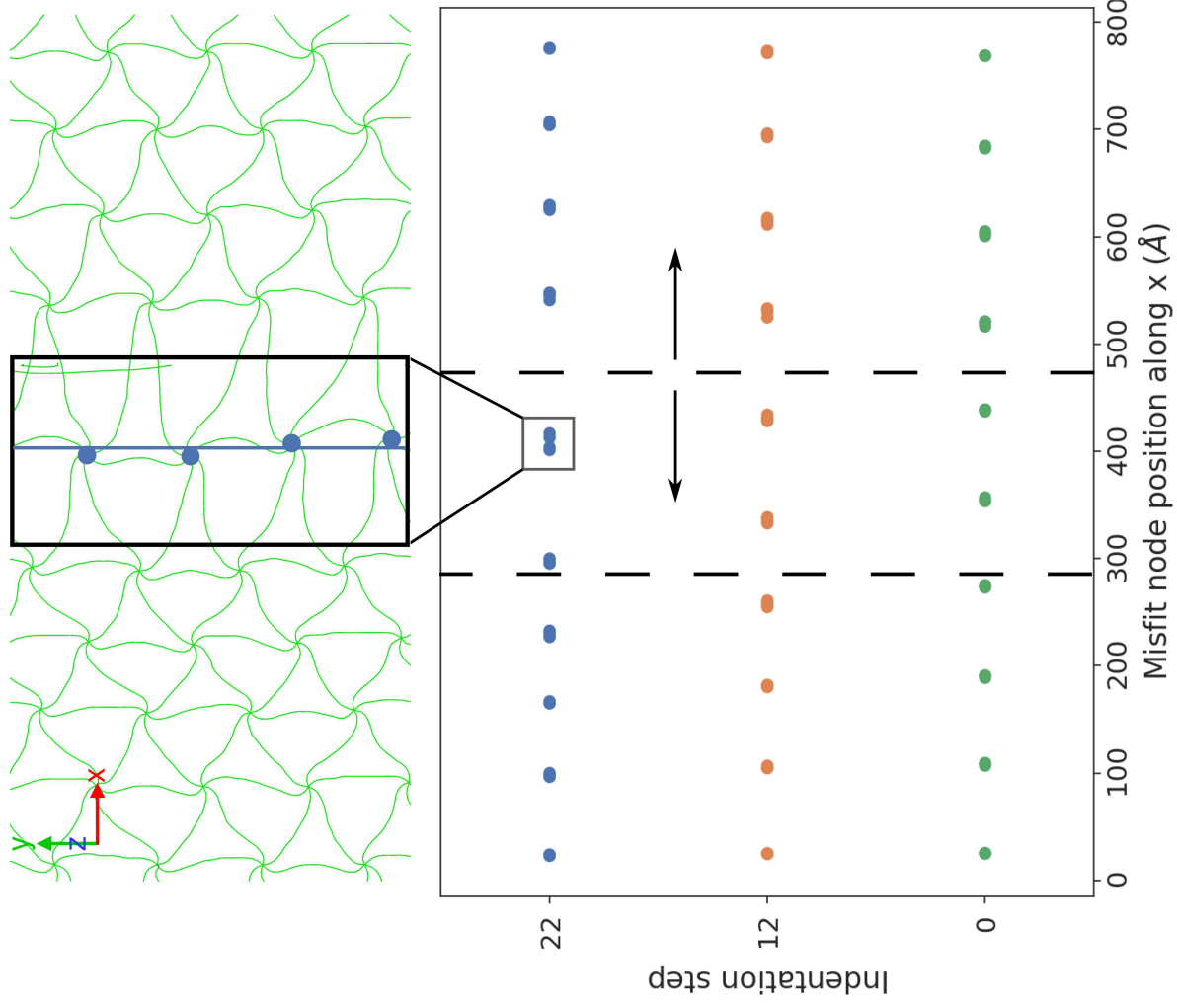
[60] G. J. Tucker, J. A. Zimmerman, and D. L. McDowell: Shear deformation kinematics of bicrystalline grain boundaries in atomistic simulations. *Modelling and Simulation in Materials Science and Engineering*.18(1), 015002 (2009).



0 Indentation Steps

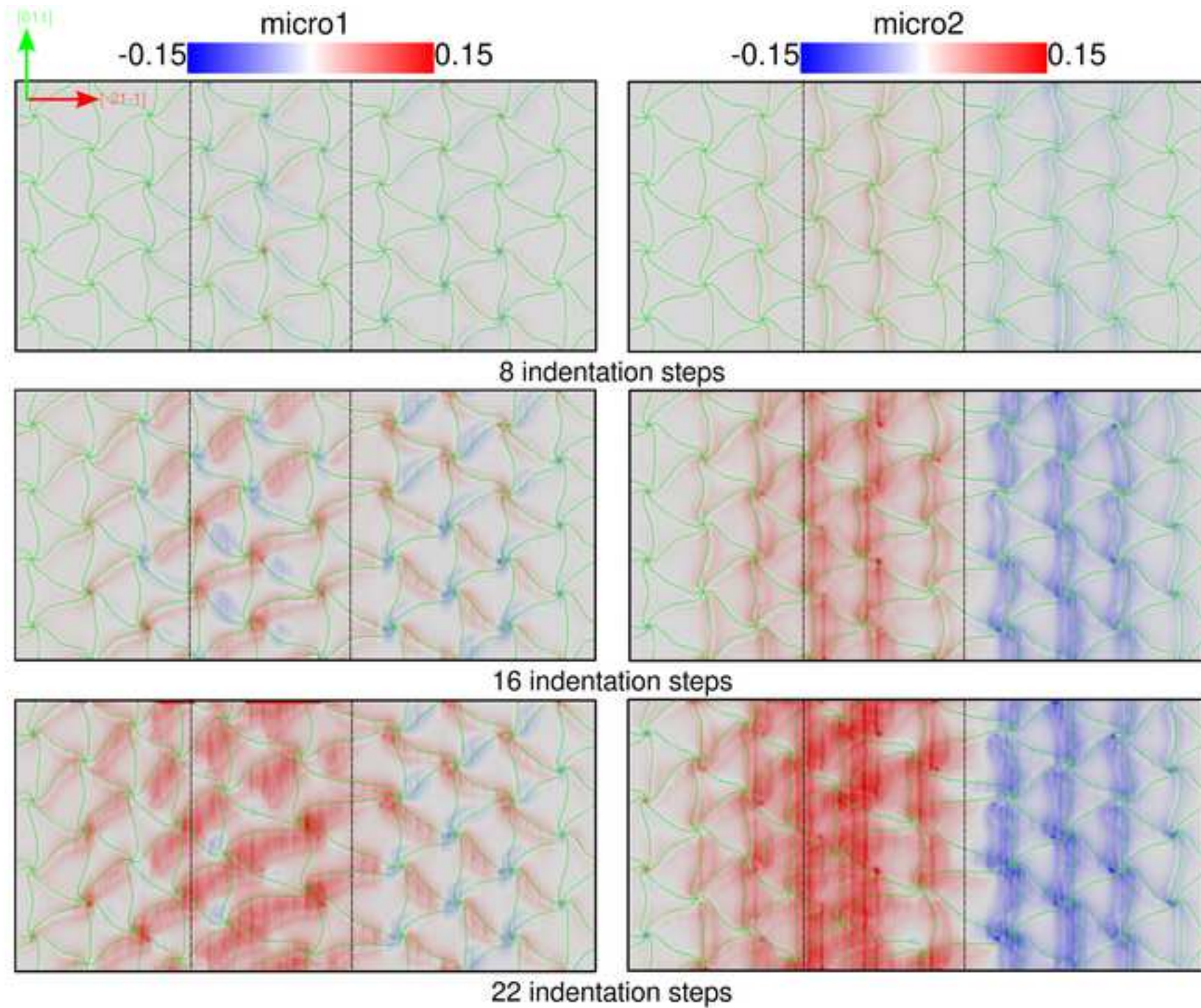


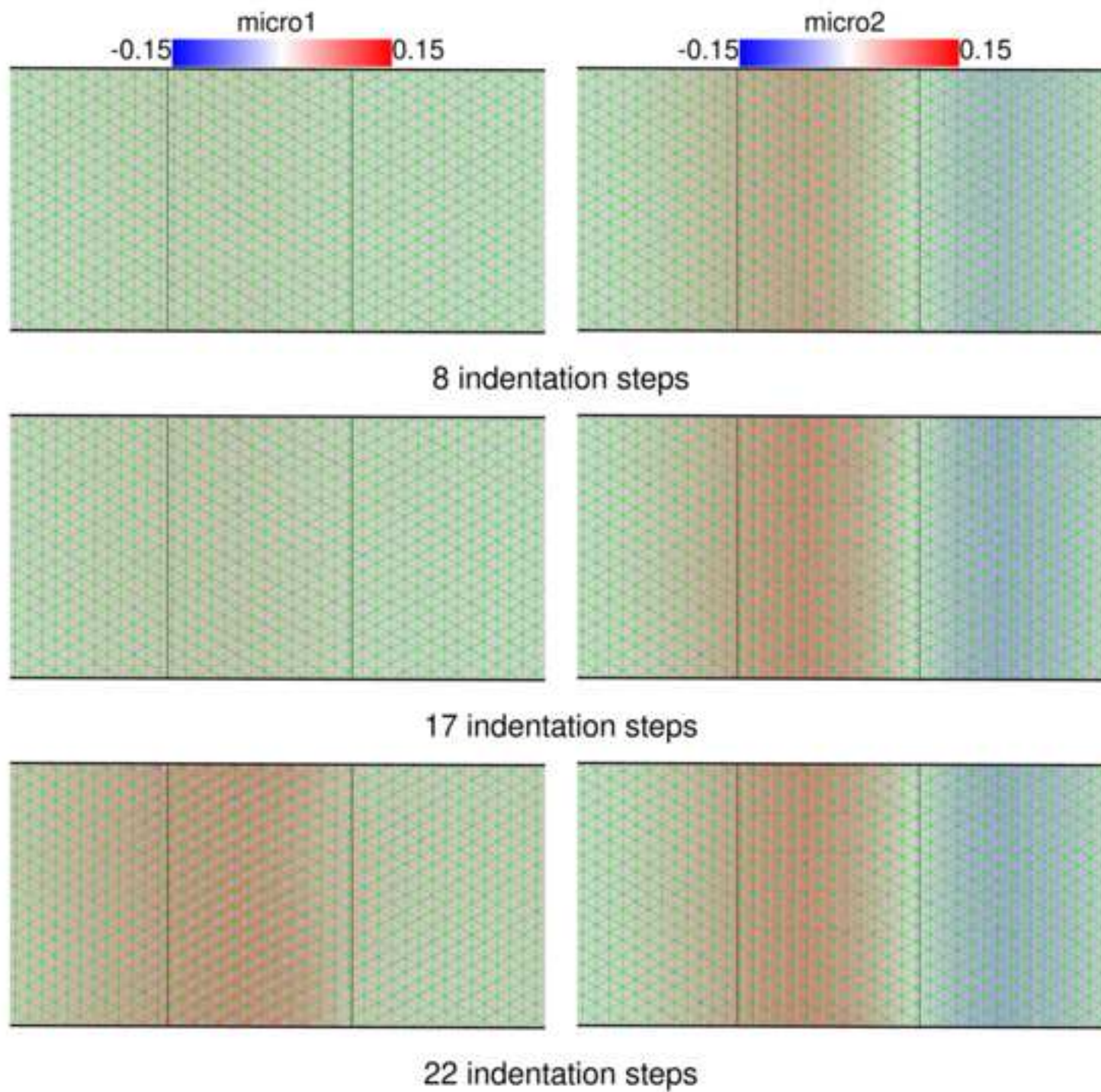
22 Indentation Steps

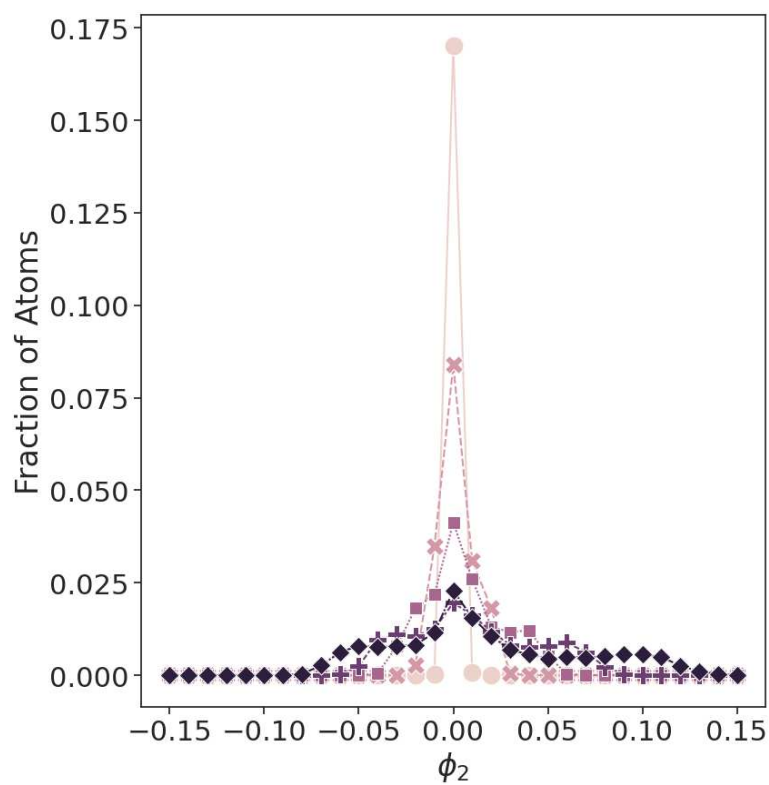
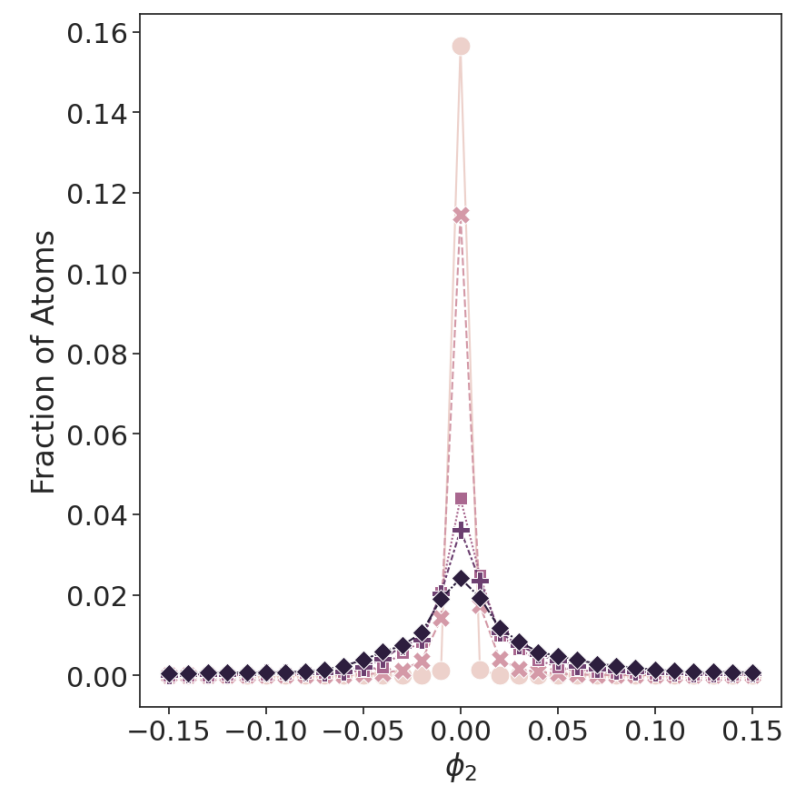
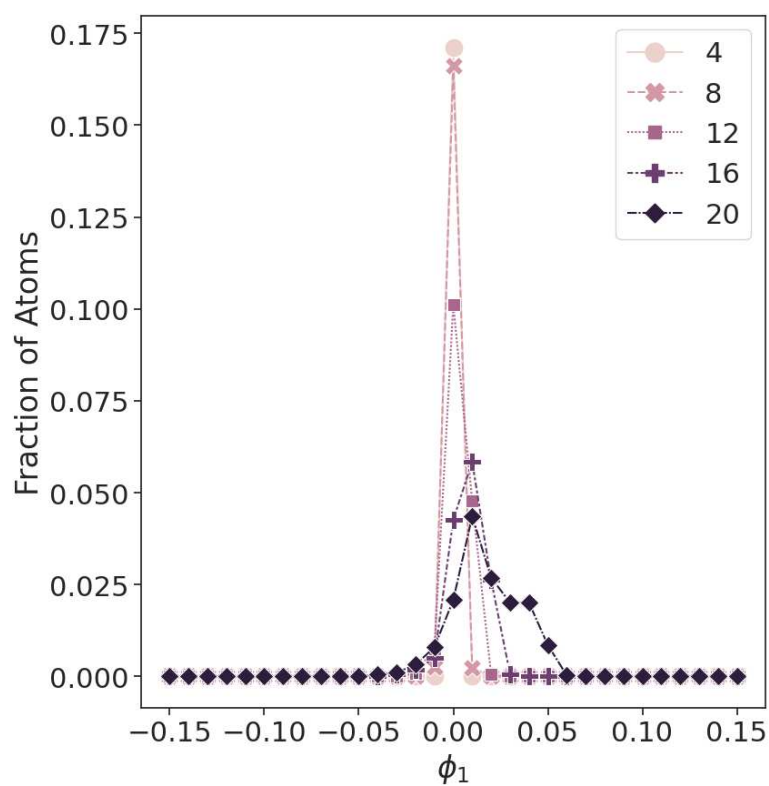
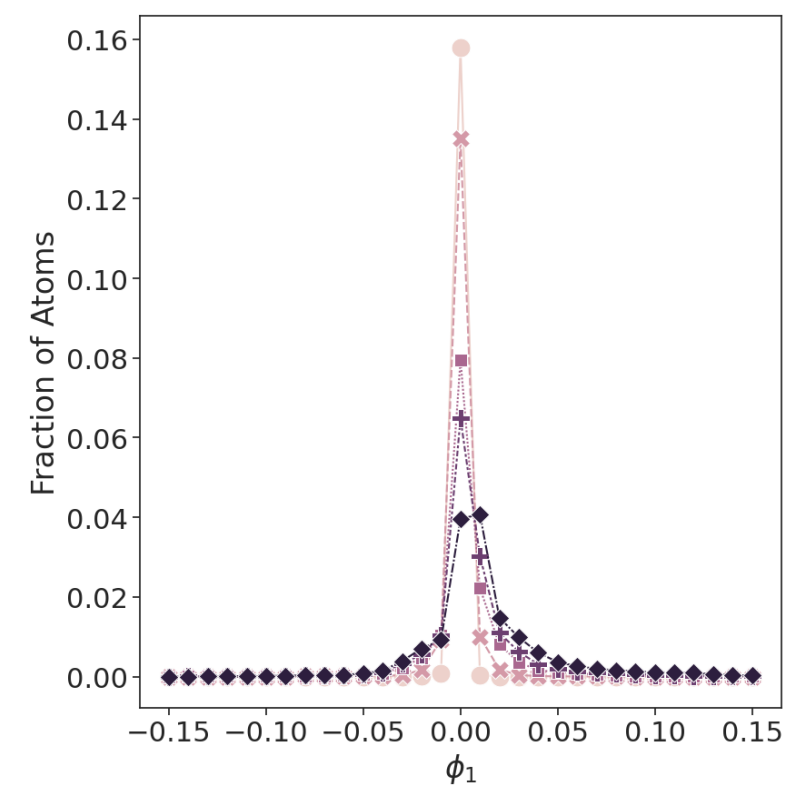


(a)

(b)



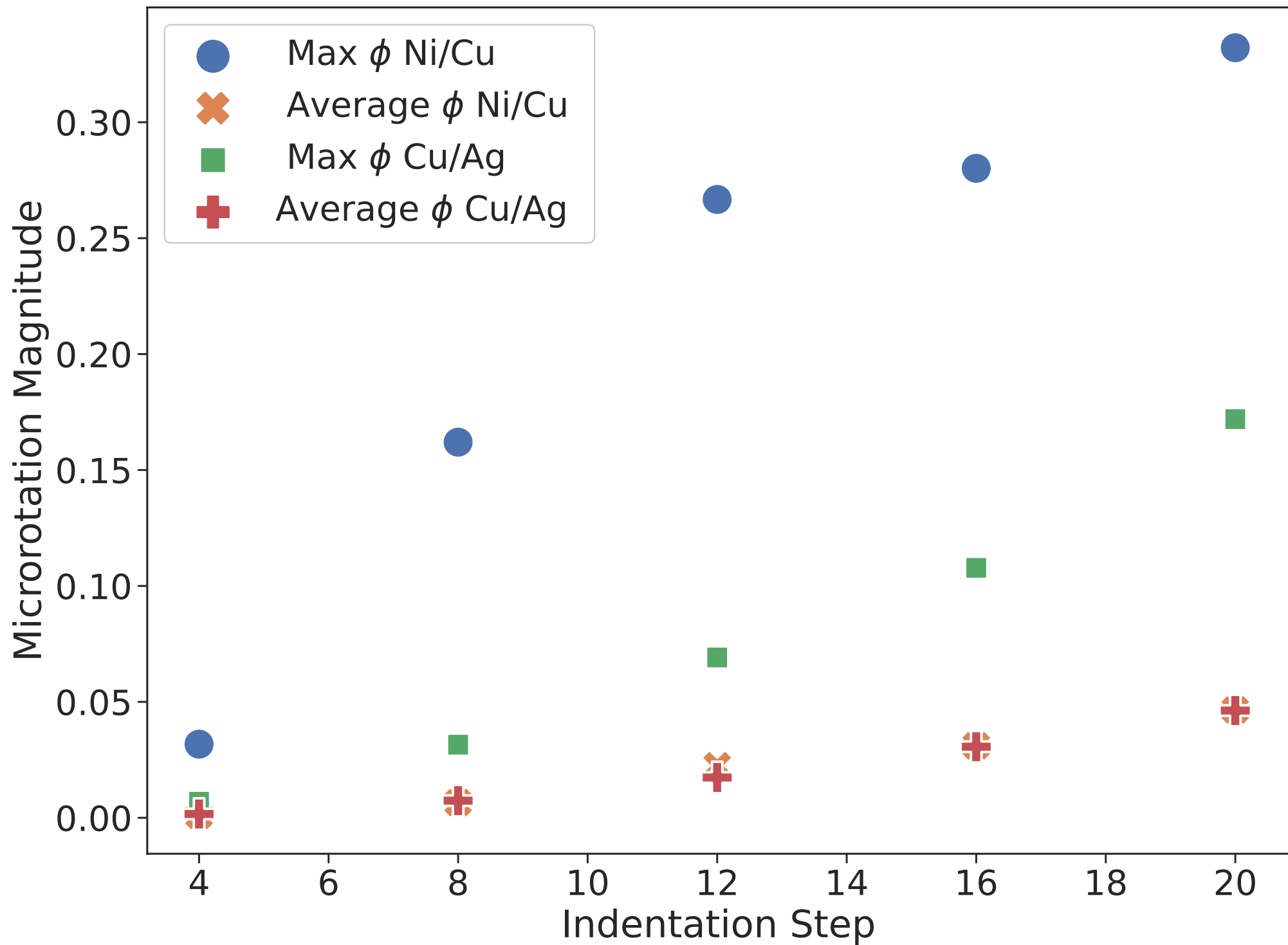


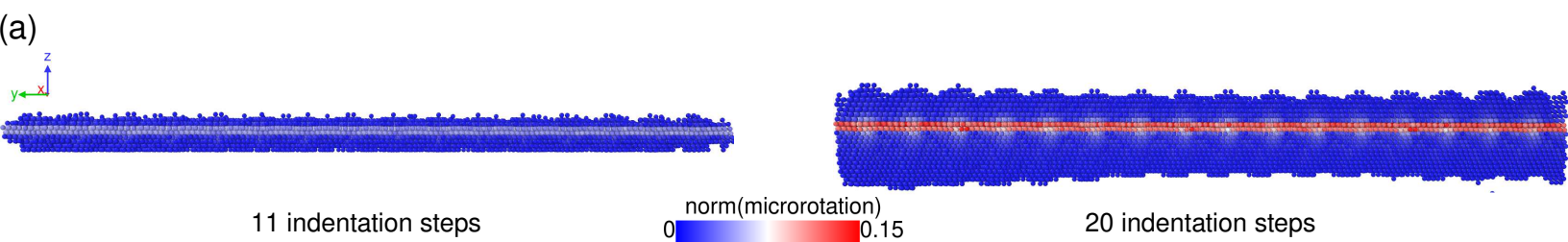
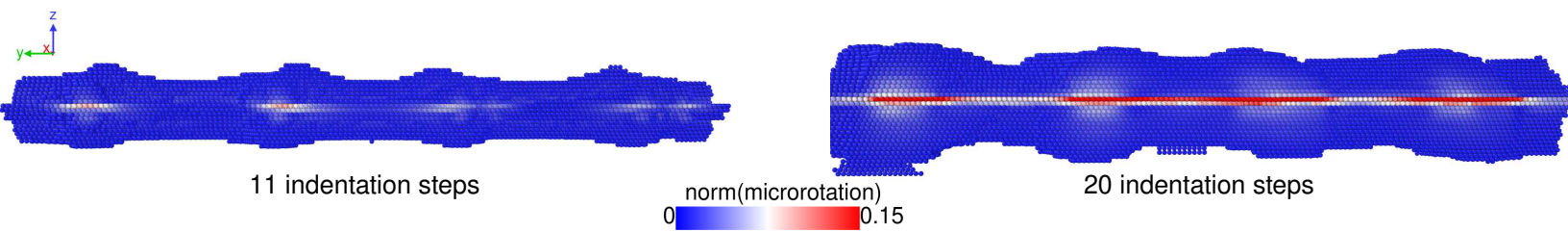


(a)

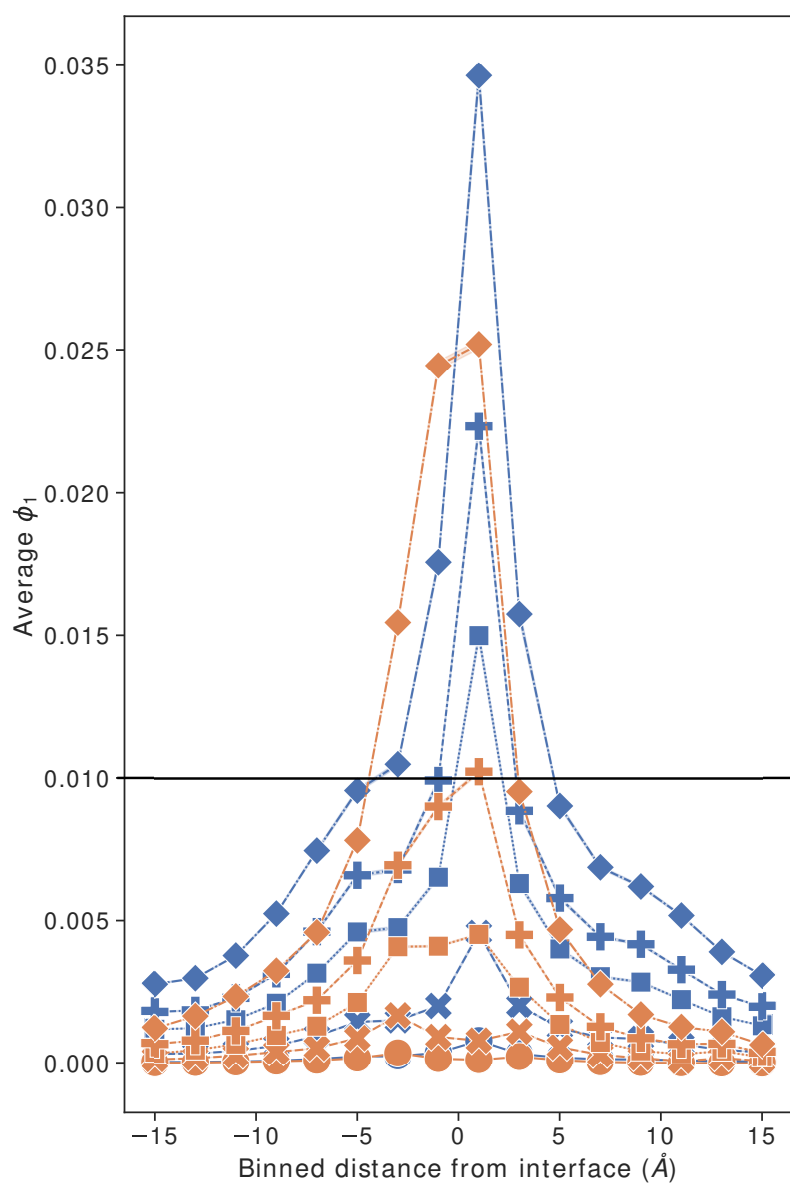
(b)



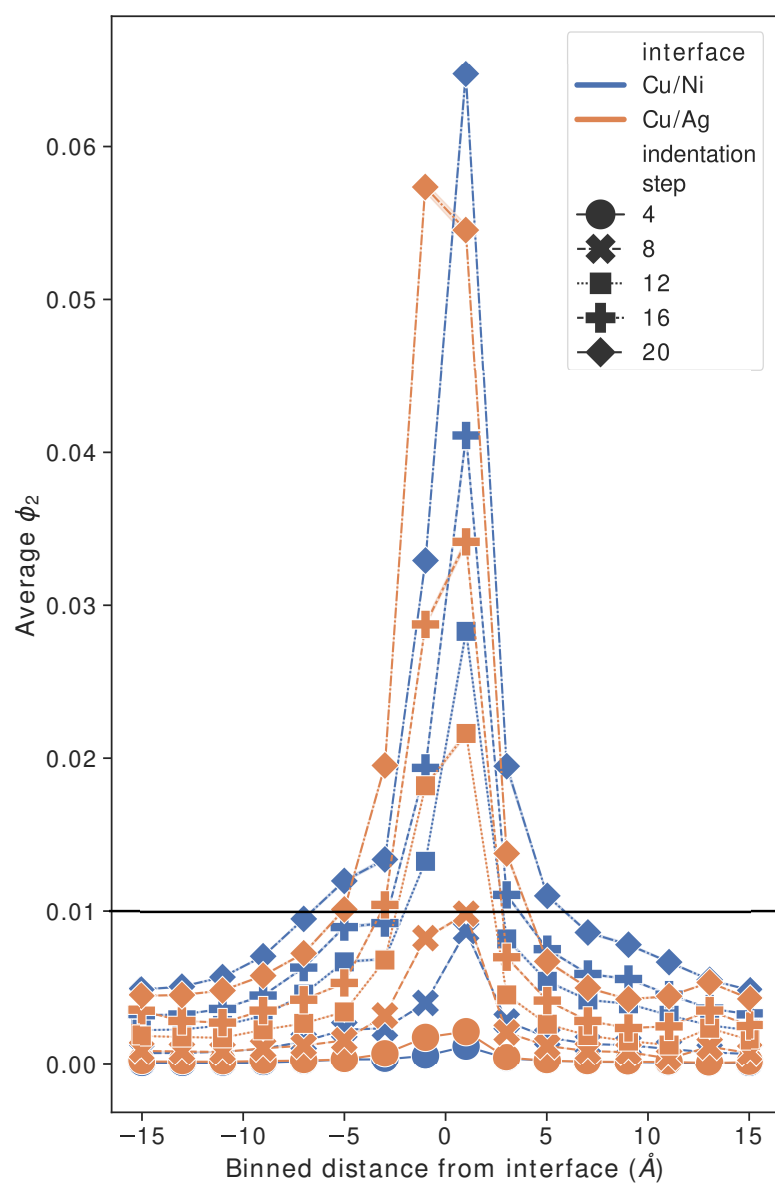




(b)



(c)



(d)

FIG 8

[Click here to access/download;Figure;Figure\\_8.eps](#)

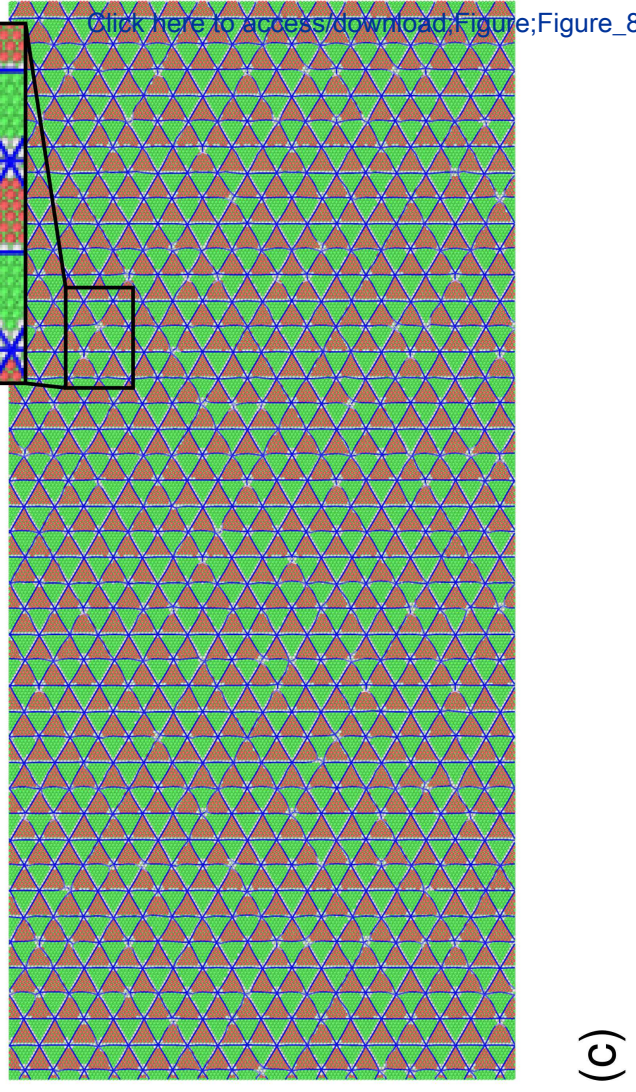
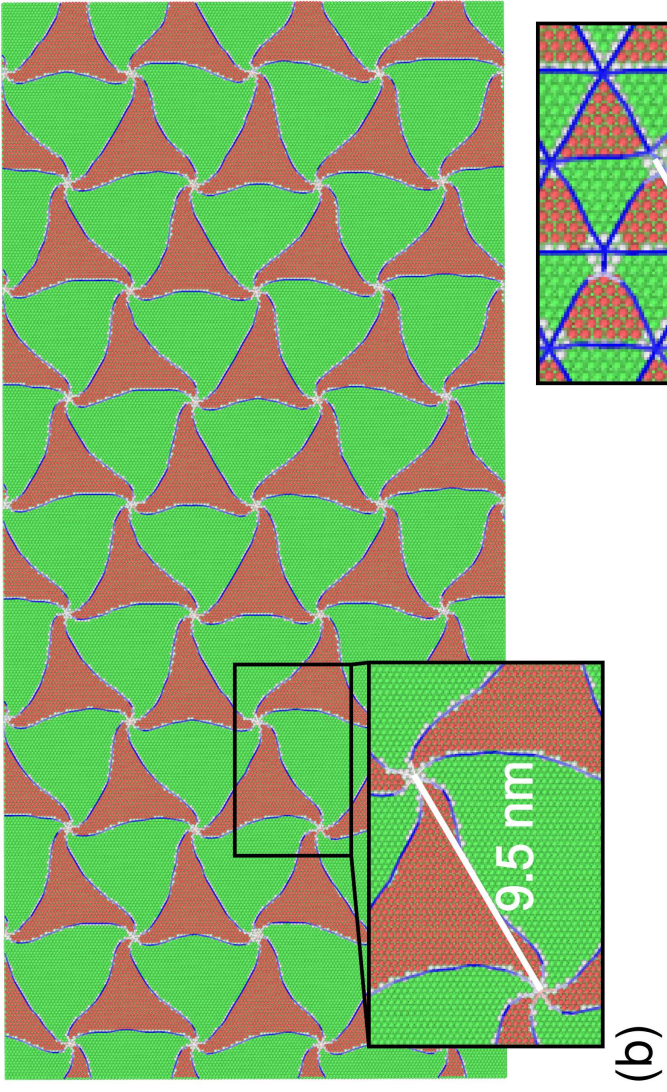
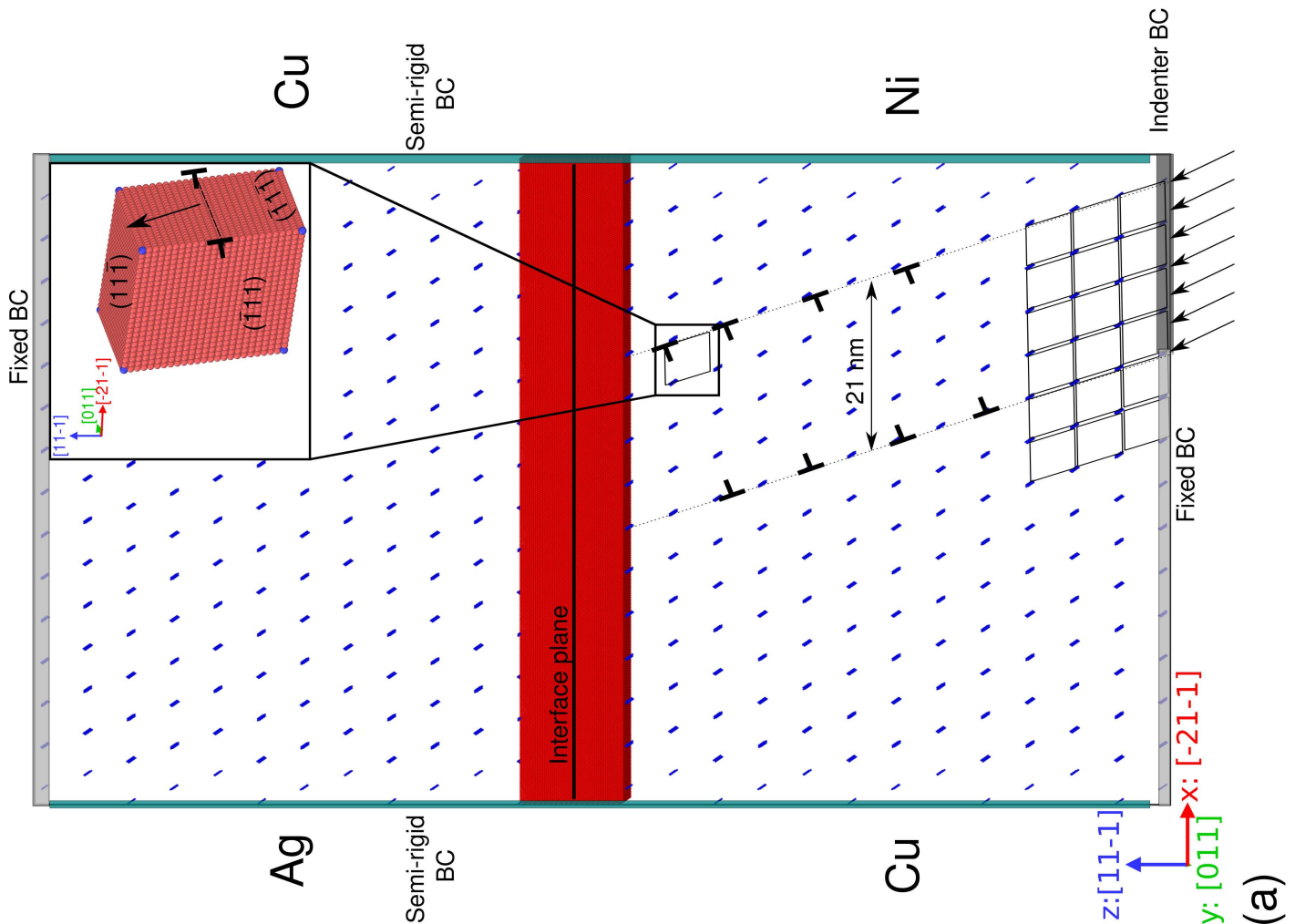
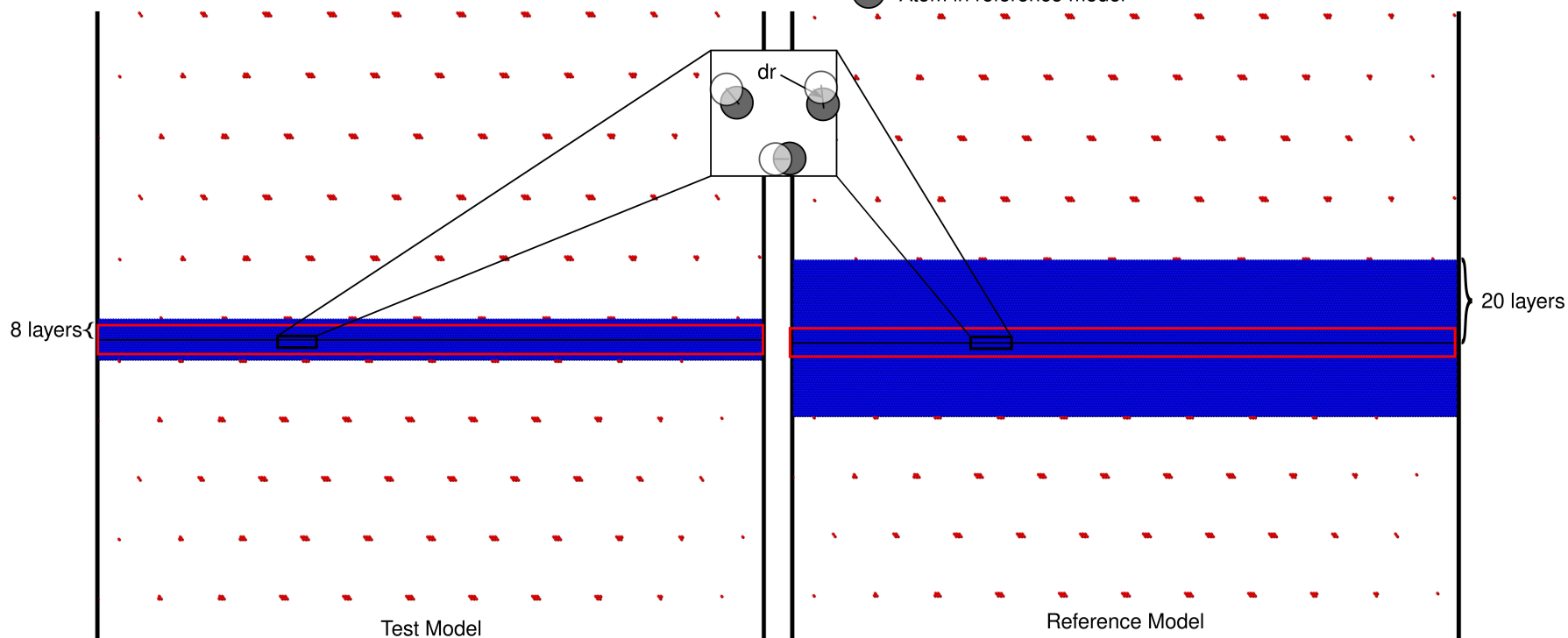


FIG 9

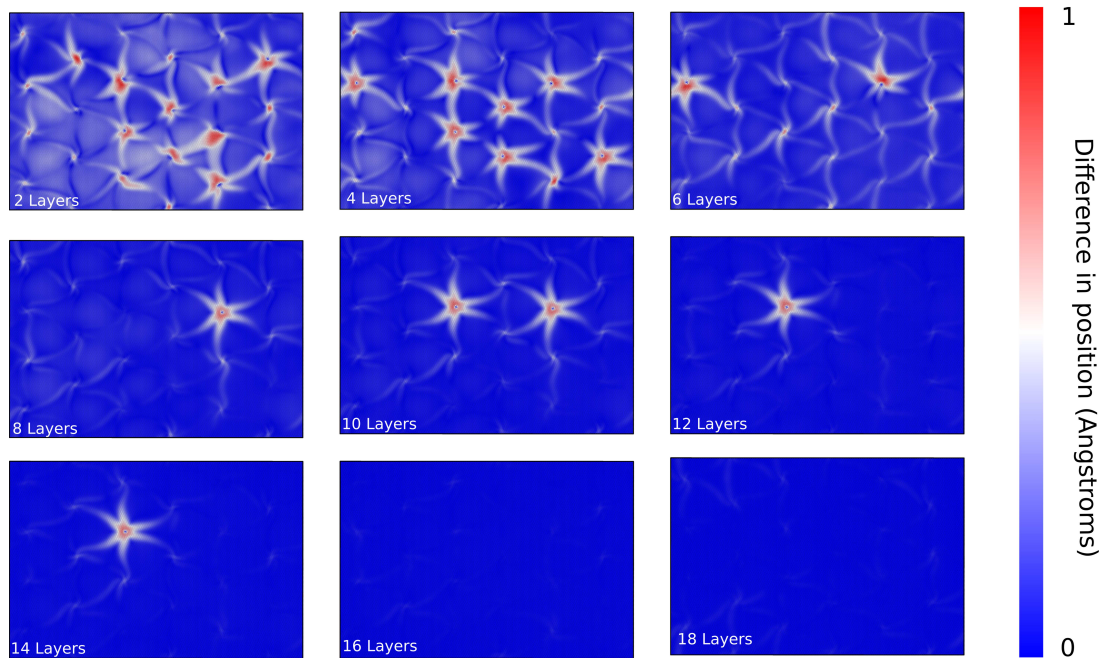
○ Atom in test model

[Click here to access/download;Figure;Figures\\_9.eps](#)

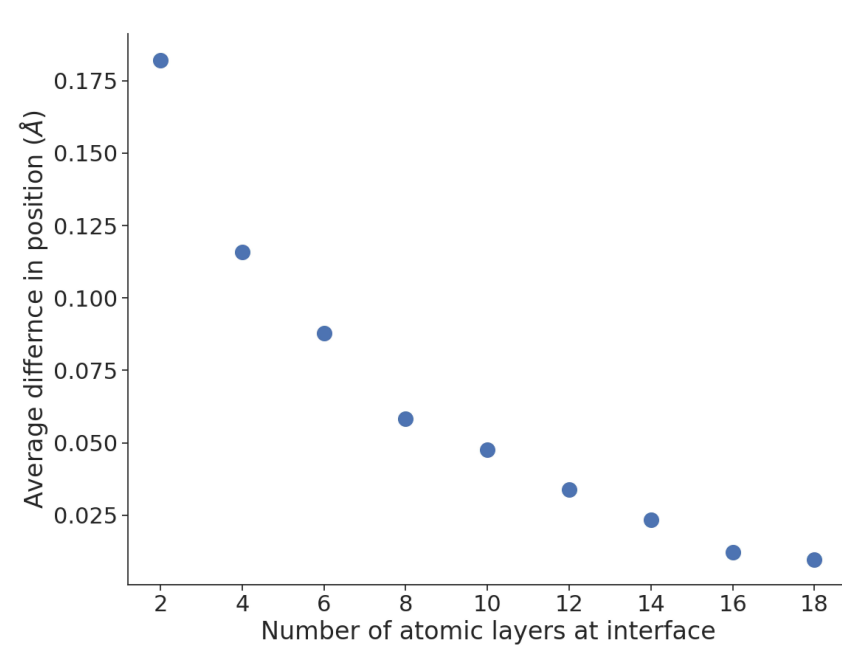
● Atom in reference model



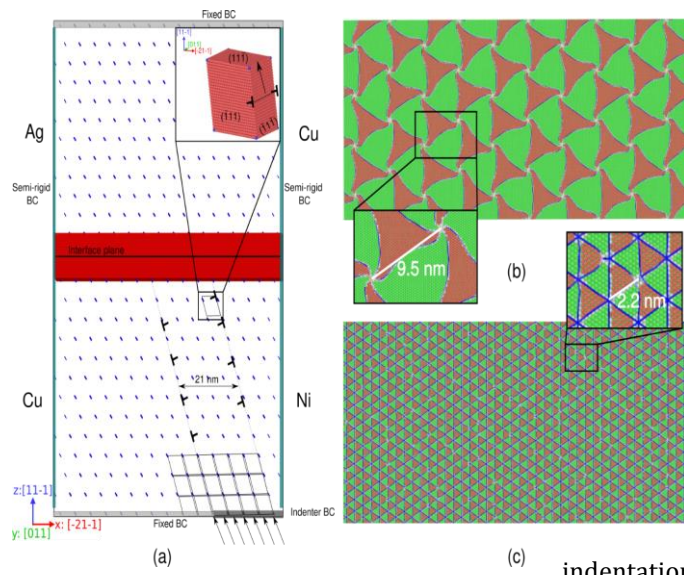
(a)



(b)



(c)



The study of dislocation plasticity mediated by semi-coherent interfaces can aid in the design of certain heterostructured materials, such as nanolaminates. The evolution of interface misfit patterns under complex stress fields arising from dislocation pileups can influence local dislocation/interface interactions, including effects of multiple incoming dislocations. This work utilizes the Concurrent Atomistic-Continuum modeling framework to probe the evolution of misfit structures at semi-coherent Ni/Cu and Cu/Ag interfaces impinged by dislocation pileups generated via nanoindentation. A continuum microrotation metric is computed at various stages of the

indentation process and used to visualize the evolution of the interface misfit dislocation pattern. The stress state from approaching dislocations induces mixed contraction and expansion of misfit dislocation structures at the interface. A lower number of misfit nodes per unit interface area coincides with greater localized deformation with regard to atoms near misfit nodes for Ni/Cu. The decreased misfit node spacing for Cu/Ag alternatively distributes the restructuring associated with plastic deformation over a larger percentage of atoms at the interface. Interface sliding facilitated by misfit dislocation motion is found to facilitate deformation extending into the bulk lattices centered on misfit nodes. The depth of penetration of those fields is found to be greater for Ni/Cu than for Cu/Ag.

## Response to Reviewers

Journal: Journal of Materials Research

Manuscript #: JMRS-D-21-00012

Title: Lattice Dislocation Induced Misfit Dislocation Evolution in Semi-Coherent {111} Bimetal Interfaces

Authors: Alex Selimov, Shuozhi Xu, Youping Chen, David L. McDowell

We appreciate the time and efforts by the editor and reviewers in reviewing this manuscript. We have addressed all issues indicated by the reviewers. Please find below our responses to reviewers in a point-by-point fashion. The revisions in the manuscript are provided in this letter and highlighted in yellow.

### Reviewer #1:

[Comment 1] The formatting of this MS is a bit strange. Please follow the layout of other published papers in this journal which used the conventional "Intro -> Methodology -> Results/discussions -> Conclusions" flow.

[Response 1] Thank you for the comment. We have read other published papers in this journal and found that the Methodology section is usually put at the end. In fact, the current formatting we use is required by the journal. Please see this webpage for the journal formatting requirement: [https://www.springer.com/journal/43578/submission-guidelines#Instructions%20for%20Authors\\_Title%20page](https://www.springer.com/journal/43578/submission-guidelines#Instructions%20for%20Authors_Title%20page)

[Comment 2] Lattice dislocations were generated using indentation. If the lattice dislocation - interface interaction is to be analyzed, the indenter needs to be far enough from the interface so that it does not affect the observations. Did the authors make sure that the effects of the indenter were excluded?

[Response 2] We thank the reviewer for this comment. Prior to running the final models, we ran two simulations with layer thicknesses of 34.5 and 65 nm for the Ni/Cu bilayer. Interface structures at the point prior to dislocation absorption into the interface were similar in both cases with the misfit node separation from the slip plane impingement differing due to the increase in induced stress from additional dislocations in the pileup. A figure describing the interface structure and a description of the figure were added. These are copied below:

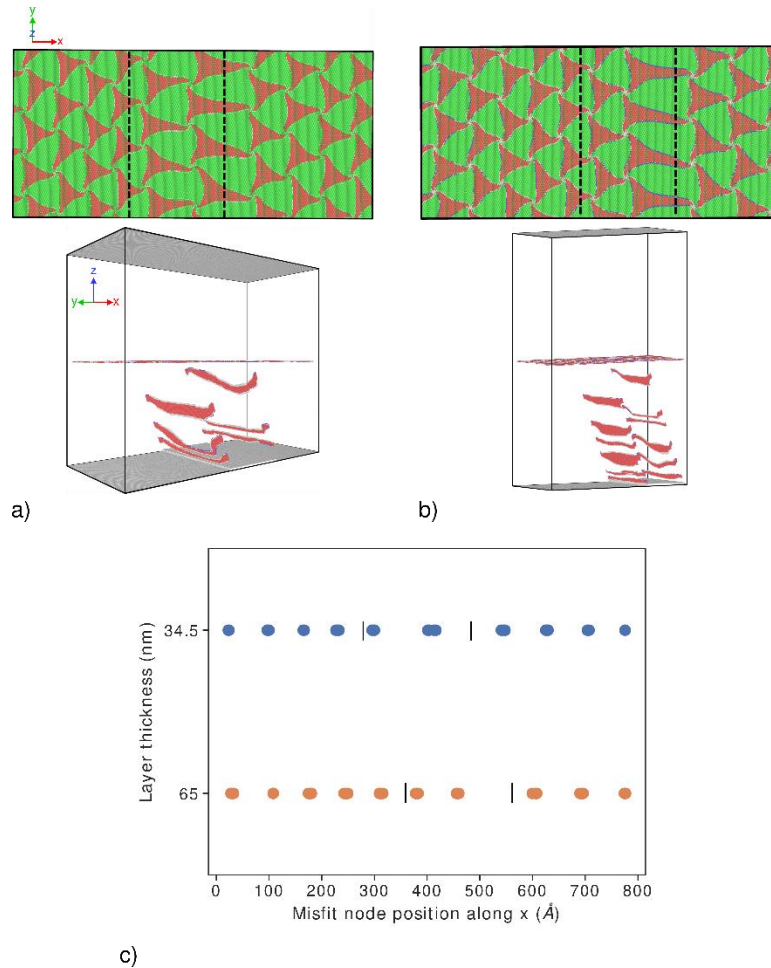


*Figure 10: a) Interface and dislocation structure for the 34.5 nm layer thickness model and b) 65 nm layer thickness model at the timestep prior to the lattice dislocation entering the interface. c) Shows the misfit node positions along the x dimension with black lines denoting the slip plane impingement sites. Similar structures are seen in both models with increased distance of misfit nodes from the impingement sites in the 65 nm model resulting from the additional shear stress imparted by the long-range fields of the additional dislocations in the pileup.*

To ensure that the indenter distance did not have a significant impact on the interface structures observed, two models with indenter distances of 34.5 nm and 65 nm from the interface were investigated. Figure 10 shows the interface structure at the indentation step prior to the dislocation entering the interface. The interface misfit structures in both cases are similar. Analysis of the node distribution along the x dimension also matches in both cases with an increased misfit node distance from the slip plane impingement for the larger model resulting from the increased shear stress induced by additional dislocations in the pileup. The 34.5 nm model was therefore selected as having sufficient separation between indenter and interface for comparing the evolution of misfit patterns for Ni/Cu and Cu/Ag.

[Comment 3] The local reorganization of the MDN observed in this work is on condition that the nodes are glissile on the interface. However, depending on the interface chemistry, the nodes may sometimes serve as pinning points to the in-plane migration of the MDN (see Zhang et al. (2017), Acta Mater., Vol. 138, Pp. 224-236). In that case, how do the authors expect the observations change?

[Response 3] We thank the reviewer for the comment. A description of expected differences in the observed structure for structures with glissile nodes was added and is copied below.

In the case of sessile misfit nodes, such as in metal/ceramic semi-coherent interfaces [40], dislocations will bow out in opposite directions, depending on the sign of the induced shear stress, with dislocation segments pinned by the misfit nodes. The degree to which the dislocations bow out will increase as additional dislocations are generated in the pileup and as they approach in the interface.

[Comment 4] Although the manuscript mentioned that slip transmission will be considered in future work, some educated guess on what to expect when/after the dislocations pass through these interfaces is still warranted. For instance, the transmission will leave interfacial ledges, which can then serve as stress concentrators and induce further emission of dislocations originated from the interface (see Dodaran et al. (2019), Acta Mater., Vol. 171, Pp. 92-107).

[Response 4] We thank the reviewer for the comment. We have included a description of what is expected for multi slip transmission and how this will differ for both Ni/Cu and Cu/Ag. These statements are based on some preliminary results that are currently being analyzed. This description is copied below.

The evolution of interface structure during sequential slip transmissions and associated changes in interface blocking strength will also be studied. The difference in Burgers vectors for both components in a bilayered material must be accommodated within the interface for slip transmission to occur which manifests as a step left on the interface. It is expected that the growth of this step will increase the interface blocking strength [41]. Increases to the blocking strength may result in a change in mechanism from slip transmission to a more favorable nucleation of dislocations from the step [42]. The increased stability of the Cu/Ag interface misfit structure and the lower misfit dislocation spacing, observed in this work, are expected to result in a higher blocking strength than that of Ni/Cu.

Reviewer #2

[Comment 1] Please describe the computation model in detail right after the introduction before entering discussion of the results.

[Response 1] We thank the reviewer for the comment. We have read other published papers in this journal and found that the Methodology section is usually put at the end. In fact, the current formatting we use is required by the journal. Please see this webpage for the journal formatting requirement: [https://www.springer.com/journal/43578/submission-guidelines#Instructions%20for%20Authors\\_Title%20page](https://www.springer.com/journal/43578/submission-guidelines#Instructions%20for%20Authors_Title%20page)

[Comment 2] Please re-write the results section. If possible, please make sub-sections to facilitate discussion. It is not clear to the reviewer what are the main findings.



[Response 2] We thank you for the comment. We have made extensive efforts to improve the readability of the results sections and to highlight main findings. As such we have followed the reviewer's suggestion to add sub-sections. Furthermore the final paragraph at the end of each sub-section contains the major findings relating to the topic being discussed.

[Comment 3] I recommend to put the figures and their captions together for the convenience of reading. Please keep in mind that the manuscript is not used for final production but only for the reviewer's evaluation. If possible, please move the figures inside the text at the right places.

[Response 3] Thank you for this comment. We have put figures together with their captions and have placed them near where they are discussed within the manuscript as per the reviewer's suggestion.

[Comment 4] A quasistatic approach is applied in the study, which does not include the thermo effects. However, dislocation/interface interaction may have strong entropic effects even at room temperature. How to justify the approach applied in the study and how valuable are the findings with regard to real applications?

[Response 4] We are grateful for the comment. Because the current work does not study the interactions of the lattice dislocations with the interfaces and instead is primarily interested in the near equilibrium evolution of the interface structure resulting from the stress fields ahead of dislocation pile ups, we deemed that quasi-statics simulations would be the best way of studying this. A discussion regarding the use of energy minimization and the real-world applications of these results was added and is copied below.

Entropic effects are not considered in this work. To study thermally activated processes, quasistatic simulations should minimally be augmented with harmonic transition state theory [39, 40] or use of the Meyer-Neldel compensation law to estimate activation entropy [41, 42] based on activation enthalpy of dislocation-interface reactions computed, for example, using nudged elastic band (NEB) methods [43]. Studying the mechanically induced misfit pattern evolution under quasi-static conditions prior to interactions with lattice dislocations can more realistically inform reduced order models, as the local misfit dislocation environment is known to affect slip transmission [17, 35] and is not too far from equilibrium. Capturing this evolution necessitates the use of large interface segments to allow for non-uniform misfit structure evolution. Important implications regarding the interface misfit structure stability and interface shear strength can furthermore aid in the design of interfaces used for hierarchically structured nanolaminates.



Department of Materials Science and Engineering  
Georgia Institute of Technology  
Atlanta, GA 30332  
E-mail: [aselimov3@gatech.edu](mailto:aselimov3@gatech.edu)  
March 6, 2021

Dear Editor,

On behalf of my co-authors Shuozhi Xu, Youping Chen, and David McDowell, I am submitting a revised manuscript entitled “Lattice Dislocation Induced Misfit Dislocation Evolution in Semi-Coherent {111} Bimetal Interfaces” to be considered for publication in the Journal of Materials Research. We confirm that this work is original and has not been published elsewhere nor is it currently under consideration for publication elsewhere. We declare no conflict of interest. We appreciate the comments from the two reviewers. In the revised manuscript, we have addressed all the reviewers' concerns and have made substantial changes. A response to reviewer letter is attached.

Understanding the evolution of bimetal interface misfit dislocation structures is critical as interest continues to grow in the exploration of nanolaminate materials. This is especially important when considering that most FCC-FCC nanolaminates will have high densities of semi-coherent interfaces when manufactured using industrial scale methods, such as Accumulative Roll Bonding, due to limitations in the minimum layer thickness that can be achieved. The evolution of misfit dislocation structures can directly impact the dislocation/interface interactions and must be quantified for accurate reduced-order modeling. One can find many studies in literature which use atomistics to model interface evolution; however, limitations due to the sizes of the models and the uniform stress states applied limit their usefulness. We utilize the Concurrent Atomistic-Continuum (CAC) method to increase the simulation cell sizes for modeling larger interface sections and their evolution when exposed to stress fields ahead of dislocation pileups generated via nanoindentation. CAC is a coarse-graining multi-scale modeling method which uses a unified atomistic-continuum integral formulation depending only on the interatomic potential to dictate model evolution. Interelement discontinuities can accommodate dislocations in coarse-grained regions and can smoothly pass them between coarse-grained and atomistic regions without the need for heuristics or other bridging methods. CAC has previously been applied to the study of interfaces with great success, as it is able to model regions near interfaces with full atomistic resolution while coarse-grained regions away from the interface reduce computational degrees of freedom and maintain large simulation domains.

In this manuscript, we apply the CAC method to study the evolution of misfit dislocation patterns in semi-coherent Cu/Ag and Ni/Cu interfaces. Nanoindentation is used on coarse-grained regions of the models to generate dislocation pileups on distinct slip planes. The evolution of the interface structure ahead of these pileups is characterized using a continuum microrotation metric which reveals additional information about reconstructive reactions associated with this evolution. Quantitative analysis of the distribution in the value of the microrotation metric reveals differences between the evolution of interface structures in Cu/Ag and Ni/Cu interfaces. Longer-range deformation fields arising from the interface deformation are also characterized numerically using the microrotation.

We believe that the presented work satisfies the stringent criteria for publication in the Journal of Materials Research due to the systemic and quantitative analysis of interface evolution. We believe that it will be of interest not only to those studying nanolaminates and bimetal interfaces, but also to researchers working generally in materials modeling due to the methods used. Please do not hesitate to contact me for any additional information that is required.

With best regards,



Alex Selimov,  
Graduate Research Assistant  
Georgia Institute of Technology, Atlanta  
<https://alexselimov.xyz>